AD_____

Award Number: DAMD17-01-1-0077

TITLE: Induced Expression of Androgen Receptor in Androgen Independent Prostate Cancer Cells Using an IkBα "Super Repressor"

PRINCIPAL INVESTIGATOR: Linda M. Kalikin, Ph.D.
Kenneth J. Pienta, M.D.

CONTRACTING ORGANIZATION: The University of Michigan
Ann Arbor, Michigan 48109-1274

REPORT DATE: September 2003

TYPE OF REPORT: Annual Summary

PREPARED FOR: U.S. Army Medical Research and Materiel Command
Fort Detrick, Maryland 21702-5012

DISTRIBUTION STATEMENT: Approved for Public Release;
Distribution Unlimited

The views, opinions and/or findings contained in this report are those of the author(s) and should not be construed as an official Department of the Army position, policy or decision unless so designated by other documentation.

Best Available Copy

20040511 024

REPORT DOCUMENTATION PAGE

Form Approved
OMB No. 074-0188

1. AGENCY USE ONLY (Leave blank)	2. REPORT DATE September 2003	3. REPORT TYPE AND DATES COVERED Annual Summary (1 Sep 02-31 Aug 03)

4. TITLE AND SUBTITLE
Induced Expression of Androgen Receptor in Androgen Independent Prostate Cancer Cells Using an IkBα "Super Repressor"

5. FUNDING NUMBERS
DAMD17-01-1-0077

6. AUTHOR(S)
Linda M. Kalikin, Ph.D.
Kenneth J. Pienta, M.D.

7. PERFORMING ORGANIZATION NAME(S) AND ADDRESS(ES)
The University of Michigan
Ann Arbor, Michigan 48109-1274

E-Mail: lkalikin@umich.edu

8. PERFORMING ORGANIZATION REPORT NUMBER

9. SPONSORING / MONITORING AGENCY NAME(S) AND ADDRESS(ES)
U.S. Army Medical Research and Materiel Command
Fort Detrick, Maryland 21702-5012

10. SPONSORING / MONITORING AGENCY REPORT NUMBER

11. SUPPLEMENTARY NOTES
Original contains color plates. All DTIC reproductions will be in black and white.

12a. DISTRIBUTION / AVAILABILITY STATEMENT
Approved for Public Release; Distribution Unlimited

12b. DISTRIBUTION CODE

13. ABSTRACT (Maximum 200 Words)

Advanced prostate cancer continues to kill 29,000 men annually in the United States. Despite strides in obtaining extended remissions through the use of hormones and chemotherapeutic agents, there is still no curative therapy for this devastating disease. While most prostate cancers are responsive to androgens and while androgen withdrawal is the main form of treatment, the failure of primary hormone therapy is attributed to androgen-independent tumor expansion. Mechanisms for the transition from androgen-sensitive to androgen-refractory disease are currently not well understood.

We proposed to investigate the role of TNF-α-mediated NF-κB signaling in androgen-sensitive and -insensitive prostate cancer, as many androgen-independent prostate cancer cell lines exhibit resistance to this pathway and as TNF-α is detected at high serum levels in relapsing prostate cancer patients compared to those in remission or untreated. We subsequently demonstrated activation of TNF-α-induced apoptosis with an IkBα super repressor and relieved NF-κB repression of the androgen receptor in androgen-independent prostate cancer cell lines cells. During this current funding period we report generation of a non-invasive quantitative murine model for metastatic prostate cancer. Thus, we now are poised to evaluate these novel insights of androgen interactions *in vivo*, a critical step toward designing novel therapeutic strategies.

14. SUBJECT TERMS
IkBα, TNF-α, CBP

15. NUMBER OF PAGES
23

16. PRICE CODE

17. SECURITY CLASSIFICATION OF REPORT Unclassified	18. SECURITY CLASSIFICATION OF THIS PAGE Unclassified	19. SECURITY CLASSIFICATION OF ABSTRACT Unclassified	20. LIMITATION OF ABSTRACT Unlimited

Table of Contents

INTRODUCTION

Advanced prostate cancer continues to kill 29,000 men per year in the United States (Jemal *et al.*, 2003). Despite strides in obtaining extended remissions in men with metastatic disease through the use of hormones and chemotherapeutic agents, there is still no curative therapy for advanced prostate cancer. While most prostate cancers are responsive to androgens and while androgen withdrawal (i.e., surgical or medical castration) is the main form of treatment for advanced (i.e. disseminated) disease, the failure of primary hormone therapy is attributed to androgen-independent tumor expansion (Pilat *et al.*, 1999). The mechanisms for the transition from androgen-sensitive to androgen-refractory disease are currently not well understood but include the development of alternative signaling pathways to circumnavigate the effects of androgen ablation, leading to reactivation of androgen-responsive genes and disease progression (reviewed in Feldman and Feldman, 2001).

A complete understanding of all culprit proteins is essential for the effective translation of molecular reagents into successful tools for the medical management of prostate cancer. Toward this end, we were intrigued by observations that many androgen-independent prostate cancer cell lines exhibit a resistance to apoptotic signaling through the apoptotic factor, tumor necrosis factor, alpha (TNF-α; Nakajima *et al.*, 1996). In addition, TNF-α is detected at high serum levels in relapsing prostate cancer patients compared to those in remission or untreated (Nakashima *et al.*, 1998). In normal cells, TNF-α initiates either an apoptotic signaling pathway or a proliferation signaling pathway depending on its cellular concentration (reviewed in Gaur and Aggarwal, 2003). At high TNF-α levels, TNF receptor is bound, and the apoptotic caspase cascade is induced. However, at low levels, TNF-α uncouples the transcription factor NF-κB cytoplasmic inhibitor IκBα. The newly released NF-κB translocates to the nucleus, binds cAMP response element binding protein (CREB)-binding protein (CBP), and induces the transcription of anti-apoptotic genes. In addition to NF-κB, the transcriptional co-regulator CBP binds other sequence-specific factors including the androgen receptor (AR; Gerritsen *et al.*, 1997) as well as different DNA binding proteins and components of the general transcription machinery (Aarnisalo *et al.*, 1998). Both NF-κB and AR require CBP for their transactivation, although CBP has a greater affinity for NF-κB than AR (Aarnisalo *et al.*, 1998). In addition, as demonstrated in our preliminary data, AR is inactive when NF-κB is active. Finally, NF-κB has been implicated in the negative regulation of the rat AR gene promoter (Supakar *et al.*, 1995). Thus, the purpose of this project is to investigate the role of TNF-α-mediated NF-κB signaling in androgen-sensitive and -insensitive prostate cancer cells.

BODY

As proposed in our approved Statement of Work, initial efforts on this project focused on engineering the prostate cancer cell lines LNCaP (PSA-producing; androgen-sensitive), PC-3 (non-PSA-producing; androgen-insensitive), and C4-2B (PSA-producing; androgen-insensitive) to express stably a PSA-IκBα "super repressor" construct. We achieved Specific Aim 1 and described in last year's Annual Report that by transfecting cells with the IκBα super repressor, TNF-α-induced apoptosis was activated (Muenchen *et al.*, 2000a) and NF-κB repression of the AR was relieved in androgen-independent prostate cancer cell lines cells (Muenchen et al, 2001a). We also showed that androgen-sensitive cells use a different caspase pathway than androgen-independent cells (Muenchen *et al.*, 2001b), suggesting that we may be able to develop better therapeutic strategies for different populations of cancer cells (Muenchen *et al.*, 2000b,

Williams *et al.*, 2000). Finally, we demonstrated that stromal and cytokine components of the tumor microenvironment mediate androgen sensitivity and cancer cell behavior (Cooper *et al.*, 2002). Thus, our early work has generated a number of novel insights into androgen interactions in hormone-sensitive and hormone-refractory prostate cancer cells which have been more recently supported by other researchers as well (Andela *et al.*, 2003).

During this past funding year, we have focused on Specific Aim 2 to generate an animal model to validate our *in vitro* results, a critical step toward advancing any agent as a potential novel therapy in the clinic. As spontaneous prostate cancer rarely occurs naturally in standard laboratory animals, metastases must be experimentally induced, most commonly by seeding immortalized human cancer cell lines into immunocompromised mice (Rosol *et al.*, 2003). More recently, these xenograft models have been improved by tagging the cell line with a chromophore before introduction into the mouse, thereby distinguishing tumor cells from host cells (Edinger *et al.*, 2002).

Using standard retroviral infection protocols, we marked the androgen- and TNF-α-insensitive prostate cancer cell line PC-3 with the bioluminescent-catalyzing enzyme luciferase (PC-3^{Luc}). Luciferase, when exposed to its substrate luciferin and in the presence of ATP, generates light in a spectral range that ideally transmits through living tissue (Rice *et al.*, 2001). Therefore, this chromophore is superior to fluorescent tags such as GFP which in contrast require an external light source for excitation that can negatively affect the quality of fluorescence produced and that can contribute to a high background, especially in deep tissue. In addition, as the luciferin/luciferase-generated biophotons are detected using a CCD camera, the same animal cohort can be repeatedly reimaged over the course of an experiment, and the same tumors can be followed unlike other models requiring weekly sacrificing from large initial experimental groups.

One week after intracardiac injection of PC-3^{LUC} cells (200,000 cells in 100 μL DPBS) into male SCID mice, anesthetized animals were injected with luciferin intraperitoneally (100 μL at 40 mg/mL) and imaged using a charge-coupled device (CCD) system at The University of Michigan In Vivo Cellular and Molecular Imaging Center (http://www.med.umich.edu/msair/). As evident by distinct bioluminescent foci, sites of micrometastases were already detectable at the liver, mandible, and hind limbs (Fig. 1; Kalikin *et al.*, 2003).

Fig 1. Luciferase tagging of PC-3 prostate cancer cells provides signposts for the location of metastatic lesions. At Week 1 on a grayscale image with pseudo-color signals overlayed, sites of metastases are evident at the liver, mandible, and hind limbs. The color bar indicates biophoton intensity levels from low (blue) to high (red). Animals are positioned on a 37°C heated platform, and nose cones deliver isofluorane anesthesia. Mice were injected with luciferin 15 min. before imaging.

All animals were imaged weekly for 6 weeks from the ventral surface and additionally at week 7 from the dorsal and lateral surfaces to aid in locating tumors. At necropsy, sites of

biophoton emissions confirmed histologically as soft tissue (Fig. 2 A, B, C) and skeletal tumors (Fig. 2 E, F, G) that corresponded to similar metastatic sites observed in advanced prostate cancer patients from our rapid autopsy program at The University of Michigan (Rubin *et al.*, 2000). In addition, tumors stained positive for luciferase expression indicating their PC-3 cell line origin (Fig 2D, H).
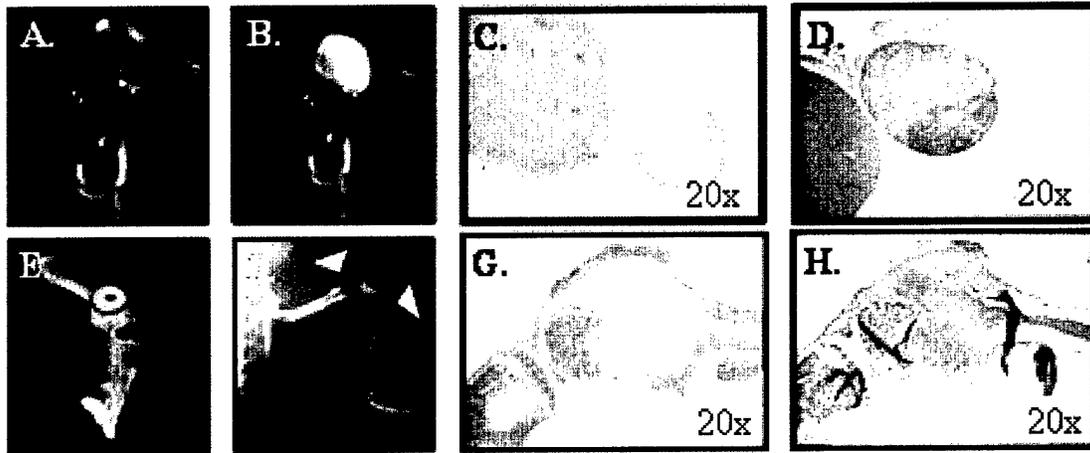

Fig. 2 *Ex vivo* analyses confirm whole animal sites of bioluminescence coincide with tumors. Representative soft tissue adrenal tumor (A.-D.) and boney tibia and femur tumors (E.-H.) are presented from two mice. Biophoton emissions are restricted to the enlarged right adrenal gland (A., B.; shown with uninvolved kidney). Tibia and femur biophoton emissions (E.) correspond to radiolucent areas on autoradiograph (F., white arrows) typical of PC-3 osteolytic lesions. Focal emissions correlate histologically with areas of blue hematoxylin-rich tumor on H&E staining (C.-adrenal; G.- hind limb). Immunohistochemical anti-luciferase staining of these tumors confirms their PC-3^{LUC} origin (D.-adrenal; H.-hind limb).

Using imaging software, photon emissions were quantified within a defined region of interest (ROI) such as an individual tumor or an entire animal. Rates of tumor growth and disease progression were then calculated by plotting against time (Fig. 3).

Fig. 3. Growth rates of tumors are determined based on quantitating photon emissions. Green ROI circles on right hind limbs are shown on ventral images of the same mouse from the last 4 weeks of a 7 week PC-3^{LUC} intracardiac injection experiment. Total photon emissions within the ROI are calculated using imaging software and plotted on the Y axis against weeks post intracardiac injection on the X axis. Histology confirmed a single femur tumor representing this bioluminescence. Grey-scale images of mice have identically scaled pseudo-color overlays.
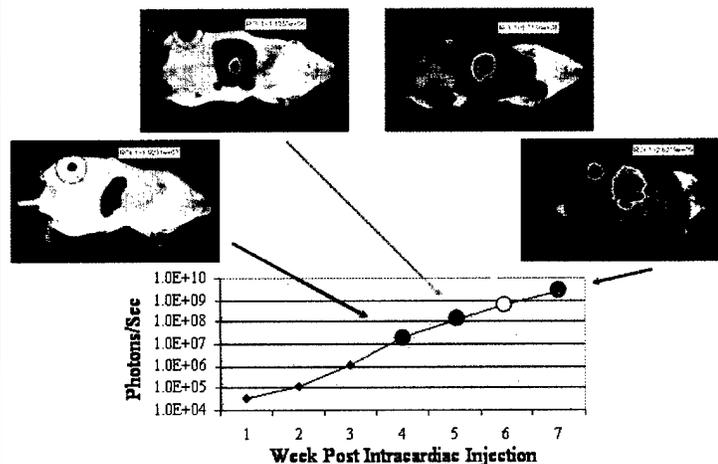
As proof-of-principal for this non-invasive, quantitative model, we then showed that individual bone tumors and disease progression occurred at a significantly faster rate in young mice compared to old mice.
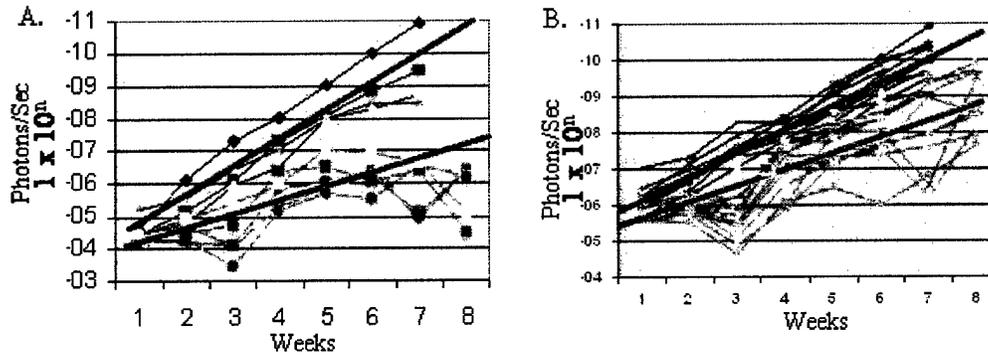

Fig. 4. Tumor growth kinetics are significantly different between young and old mice. Individual bone tumors (A.; black lines) and total tumor burden (B.; blue lines) grow significantly faster ($p < 0.001$ for both) in young mice (7 weeks old at intracardiac injection) compared to old mice (green lines; 12 months old at intracardiac injection). This is visualized as steeper slopes on graphs of photon emissions/sec (Y axis) vs weeks post-intracardiac injection (X axis). Bone tumors represent tibia, femur or mandible sites. Total tumor burden is calculated from ROIs encompassing the entire animal. Red lines represent mean regression calculations.

KEY RESEARCH ACCOMPLISHMENTS

- Generation of a sensitive, non-invasive murine model that uses luciferase as an optical reporter for tumor location and mimics clinically observed tumors in early to late state metastatic prostate cancer.
- Demonstration of the ability to assess empirically tumor growth rates and disease progression.
- Substantiation of our earlier observations that tumor microenvironment mediates cancer cell behavior (Cooper et al., 2002) based on our calculated faster tumor growth and disease progression in younger mice who possess more circulating growth factors compared to rates in aged mice.
- Generation of an in vivo model with which to evaluate the PSA-IκBα "super repressor" construct.

REPORTABLE OUTCOMES

The manuscripts and abstracts listed below reflect the work accomplished with the support of this award. Investigator names are in bold indicating those Reportable Outcomes generated since the last Annual Report and are included in the Appendix. In addition, this award served as a springboard to a tenure track position for Dr. Cooper as an Assistant Professor of Biological Sciences at the University of Delaware-Newark. Personnel who have received pay from this research effort are:

Heather Muenchen, Ph.D. – Investigator
Carlton R. Cooper, Ph.D. – Investigator
Linda M. Kalikin, Ph.D.- Investigator
Kenneth J. Pienta, M.D. – Project Mentor

7

Manuscripts

Muenchen, H.J., Lin, D.L., Walsh, M.A., Keller, E.T., Pienta, K.J. Tumor necrosis factor-alpha-induced apoptosis in prostate cancer cells through inhibition of nuclear factor-kappaB by an I kappa B alpha "super repressor." Clin Cancer Res 6:1969-77, 2000.

Muenchen, H.J., Quigley, M.M., Pilat, M.J., Lehr, J.E., Brumfield, S.K., Mahoney, M., Pienta, K.J. The study of gemcitabine in combination with other chemotherapeutic agents as an effective treatment for prostate cancer. Anticancer Research 20:735-40, 2000.

Williams, J.F., Muenchen, H.J., Kamradt, J.M., Korenchuk, S., Pienta, K.J. Treatment of androgen-independent prostate cancer using antimicrotubule agents docetaxel and estramustine in combination: an experimental study. The Prostate 44:275-278, 2000.

Muenchen, H.J., Poncza, P.J., Pienta, K.J. Different docetaxel-induced apoptotic pathways are present in prostate cancer cell lines LNCaP and PC-3. Urology 57:366-370, 2001.

Cooper, C.R., Bhatia, J.K., Muenchen, H.J., McLean, L., Hayasaka, S., Taylor, J., Poncza, P.J., Pienta, K.J. The regulation of prostate cancer cell adhesion to human bone marrow endothelial cell monolayers by androgen dihydrotestosterone and cytokines. Clin Exp Metastasis 19:25-33, 2002.

Lee, H.L., Pienta, K.J., Kim, W.J., **Cooper, C.R.** The effect of bone-associated growth factors and cytokines on the growth of prostate cancer cells derived from soft tissue versus bone metastases in vitro. Int J Oncol 22:921-926, 2003.

Kalikin, L.M., Schneider, A., Thakur, M.A., Fridman, Y., Griffin, L.B., Dunn, R.L., Rosol, T.J., Shah, R.B., Rehemtulla, A., McCauley, L.K., Pienta, K.J. In vivo visualization of metastatic prostate cancer and quantitation of disease progression in immunocompromised mice. Cancer Bio Ther 2:17-21, 2003.

Abstracts

Muenchen, H.J., Linn, D.L., Walsh, M.A., Keller, E.T., Pienta, K.J. Expression of clusterin in androgen independent prostate cancer cells after transfection with an IκBα "Super-Repressor." Proc AACR 41:4045, 2000.

Muenchen, H.J., Lin, D.L., Walsh, M.A., Keller, E.T., Pienta, K.J. TNF-alpha insensitive prostate cancer cells experience apoptosis when transfected with an IkBa "super repressor." Proc AUA 163:436a, 2000.

Cooper, C.R., Bhatia, J., Muenchen, H.J., McLean, L., Poncza, P., Pienta, K.J. The role of androgen and cytokines in prostate cancer cell adhesion to human bone marrow endothelial cell monolayers. Proc AACR 42:774, 2001.

Muenchen, H.J., Lin, D.L., Gendernalik, J.D., Keller, E.T., Pienta, K.J. Repression of androgen receptor in androgen-sensitive LNCaP prostate cancer cells through inhibition of NF-kB. Proc AACR 42:2313, 2001.

Muenchen, H.J., Lin, D.L., Poncza, P., McLean, L.L., Dirette, M.L., Keller, E.T., Pienta, K.J. Functional androgen receptor re-expression in androgen-independent prostate cancer cells. Proc AACR 42:674, 2001.

Muenchen, H.J., Poncza, P.J., Pienta, K.J. Docetaxel induces different apoptotic pathways in prostate cancer cells LNCaP and PC-3. Proc AACR 42:2331, 2001.

Muenchen, H.J., Lin, D.L., Poncza, P.J., McLean, L.L., Dirette, M.L., Keller, E.T., Pienta, K.J. Renewed sensitivity to androgen and anti-androgen in androgen-independent prostate cancer cells through re-expression of androgen receptor by an IkB "Super-Repressor." Proc AUA 165:179, 2001.

Muenchen, H.J., Lin, Gendernalik, J.J., Keller, E.T., Pienta, K.J. Inhibition of NF-kB blocks IGFBP-2 transcription and results in repression of androgen receptor in androgen-sensitive LNCAP prostate cancer cells. Proc AUA 165:196, 2001.

Kalikin, L.M., Schneider, A., Griffin, L.B., Rehemtulla, A., McCauley, L.K., Pienta, K.J. Intracardiac injection of luciferase-expressing PC-3 generates a non-invasive in vivo model of metastatic prostate cancer progression in immunocompromised mice. American Association for Cancer Research 94th Annual Meeting, 2003.

Kalikin, L.M., Schneider, A., Griffin, L.B., Rehemtulla, A., McCauley, L.K., Pienta, K.J. In vivo visualization and quantitation of metastatic bone disease progression in SCID mice. American Society for Bone and Mineral Research 25th Annual Meeting, 2003.

CONCLUSIONS

This has been a highly successful award that has resulted in key discoveries related to androgen receptor function and sensitivity to chemotherapy. Our bioluminescent murine metastatic prostate cancer model is ideal to investigate the *in vivo* effects of the PSA-IκBα super repressor on NF-κB and androgen receptor signaling as proposed in Specific Aim 3 of this project.

REFERENCES

Aarnisalo, P., Palvimo, J.J., Janne, O.A. CREB-binding protein in androgen receptor-mediated signaling. PNAS USA 95:2122-2127, 1998.

Andela, V.B., Gordon, A.H., Zotalis, G., Rosier, R.N., Goater, J.J., Lewis, G.D., Schwarz, E.M., Puzas, J.E., O'Keefe, R.J. NFkappaB: a pivotal transcription factor in prostate cancer metastasis to bone. Clin Orthop. 415 Suppl:S75-S85, 2003.

Cooper, C.R., Bhatia, J.K., Muenchen, H.J., McLean, L., Hayasaka, S., Taylor, J., Poncza, P.J., Pienta, K.J. The regulation of prostate cancer cell adhesion to human bone marrow endothelial cell monolayers by androgen dihydrotestosterone and cytokines. Clin Exp Metastasis 19:25-33, 2002.

Edinger, M., Cao, Y.A., Hornig, Y.S., Jenkins, D.E., Verneris, M.R., Bachmann, M.H., Negrin, R.S., Contag, C.H. Advancing animal models of neoplasia through in vivo bioluminescence imaging. Eur J Cancer 38:2128-2136, 2002.

Gerritsen, M.E., Williams, A.J., Neish, A.S., Moore, S., Shi, Y., Collins, T. CREB-binding protein/p300 are transcriptional coactivators of p65. PNAS USA 94:2927-2932, 1997.

Gaur, U., Aggarwal, B.B. Regulation of proliferation, survival and apoptosis by members of the TNF superfamily. .Biochem Pharmacol. 66:1403-1408, 2003.

Jemal, A., Murray, T., Samuels, A., Ghafoor, A., Ward, E., Thun, M.J. Cancer statistics, 2003. CA Cancer J Clin 2003: 53: 5-26.

Kalikin, L.M., Schneider, A., Thakur, M.A., Fridman, Y., Griffin, L.B., Dunn, R.L., Rosol, T.J., Shah, R.B., Rehemtulla, A., McCauley, L.K., Pienta, K.J. In vivo visualization of metastatic prostate cancer and quantitation of disease progression in immunocompromised mice. Cancer Bio Ther 2:17-21, 2003.

Muenchen, H.J., Lin, D.L., Walsh, M.A., Keller, E.T., Pienta, K.J. Tumor necrosis factor-alpha-induced apoptosis in prostate cancer cells through inhibition of nuclear factor-kappaB by an I kappa B alpha "super repressor." Clin Cancer Res 6:1969-77, 2000a.

Muenchen, H.J., Quigley, M.M., Pilat, M.J., Lehr, J.E., Brumfield, S.K., Mahoney, M., Pienta, K.J. The study of gemcitabine in combination with other chemotherapeutic agents as an effective treatment for prostate cancer. Anticancer Research 20:735-40, 2000b.

Muenchen, H.J., Lin, D.L., Gendernalik, J.D., Keller, E.T., Pienta, K.J. Repression of androgen receptor in androgen-sensitive LNCaP prostate cancer cells through inhibition of NF-kB. Proc AACR 42:2313, 2001a.

Muenchen, H.J., Poncza, P.J., Pienta, K.J. Different docetaxel-induced apoptotic pathways are present in prostate cancer cell lines LNCaP and PC-3. Urology 57:366-370, 2001b.

Nakajima, Y., DelliPizzi, A.M., Mallouh, C., Ferreri, N.R. TNF-mediated cytotoxicity and resistance in human prostate cancer cell lines. Prostate 29:296-302, 1996.

Nakashima, J., Tachibana, M., Ueno, M., Miyajima, A., Baba, S. Association between tumor necrosis factor in serum and cachexia in patients with prostate cancer. Clin Cancer Res 4:1743-1748, 1998.

Pilat, M.J., Kamradt, J.M., Pienta, K.J. Hormone resistance in prostate cancer. Cancer Metastasis Rev 17:373-381, 1998.

Rice, B.W., Cable, M.D., Nelson, M.B. In vivo imaging of light-emitting probes. J Biomed Opt 6:432-440, 2001.

Rosol, T.J., Tannehill-Gregg, S.H., LeRoy, B.E., Mandl, S., Contag, C.H. Animal models of bone metastasis. Cancer 97:748-757, 2003.

Rubin, M.A., Putzi, M., Mucci, N., Smith, D.C., Wojno, K., Korenchuk, S., Pienta, K.J. Rapid ("warm") autopsy study for procurement of metastatic prostate cancer. Clin Cancer Res 6:1038-1045, 2000.

Supakar, P.C., Jung, M.H., Song, C.S., Chatterjee, B., Roy, A.K. Nuclear factor kappa B functions as a negative regulator for the rat androgen receptor gene and NF-kappa B activity increases during the age-dependent desensitization of the liver. J Biol Chem 270:837-842, 1995.

Williams, J.F., Muenchen, H.J., Kamradt, J.M., Korenchuk, S., Pienta, K.J. Treatment of androgen-independent prostate cancer using antimicrotubule agents docetaxel and estramustine in combination: an experimental study. The Prostate 44:275-278, 2000.

APPENDICES (attached)

Lee, H.L., Pienta, K.J., Kim, W.J., Cooper, C.R. The effect of bone-associated growth factors and cytokines on the growth of prostate cancer cells derived from soft tissue versus bone metastases in vitro. Int J Oncol 22:921-926, 2003.

Kalikin, L.M., Schneider, A., Thakur, M.A., Fridman, Y., Griffin, L.B., Dunn, R.L., Rosol, T.J., Shah, R.B., Rehemtulla, A., McCauley, L.K., Pienta, K.J. In vivo visualization of metastatic prostate cancer and quantitation of disease progression in immunocompromised mice. Cancer Bio Ther 2:17-21, 2003.

Kalikin, L.M., Schneider, A., Griffin, L.B., Rehemtulla, A., McCauley, L.K., Pienta, K.J. Intracardiac injection of luciferase-expressing PC-3 generates a non-invasive in vivo model of metastatic prostate cancer progression in immunocompromised mice. American Association for Cancer Research 94th Annual Meeting, 2003.

Kalikin, L.M., Schneider, A., Griffin, L.B., Rehemtulla, A., McCauley, L.K., Pienta, K.J. In vivo visualization and quantitation of metastatic bone disease progression in SCID mice. American Society for Bone and Mineral Research 25th Annual Meeting, 2003.

APPENDIX 1

The effect of bone-associated growth factors and cytokines on the growth of prostate cancer cells derived from soft tissue versus bone metastases *in vitro*

HYUNG-LAE LEE[1], KENNETH J. PIENTA[2], WUN-JAE KIM[1] and CARLTON R. COOPER[2]

[1]Chungbuk National University, Cheongju, Korea; [2]University of Michigan, Ann Arbor, MI, USA

Abstract. Prostate cancer metastasis to bone may be mediated by preferential proliferation of these cells in the bone's microenvironment. We hypothesize that this preferential proliferation is mediated by bone-associated growth factors (GFs) and cytokines. To test our hypothesis, human prostate cancer cells, derived from both soft tissue (LNCaP, DuCaP, DU145) and bone metastases (PC-3, VCaP, MDA-2a, MDA-2b), were treated with bone-associated GFs and cytokines (PDGF, IGF-1, TGF-ß, EGF, bFGF, TNF-α, IL-1, and IL-6) for 48 h, and their growth responses were compared. The responses of soft tissue-derived prostate cancer cell lines to bone GFs and cytokines were variable. LNCaP cell growth was stimulated by IGF-1 but was inhibited by TNF-α. DU145 cell growth was stimulated with EGF. Prostate cancer cell lines derived from bone metastases also responded variably to bone GFs and cytokines. IL-1 stimulated the growth of MDA-2a and 2b cell lines in a dose-dependent manner. PDGF and bFGF both demonstrated variable effects on bone-derived prostate cancer cell lines. TNF-α inhibited proliferation of the VCaP cells. These findings demonstrate that human prostate cancer cell lines derived from bone metastases may not respond preferentially to bone-associated GFs and cytokines.

Introduction

Prostate adenocarcinoma (PCa) is consistently recognized as the second leading cause of cancer death in North American

Correspondence to: Dr Carlton R. Cooper, Department of Internal Medicine, University of Michigan Medical School, 1500 East Medical Center Dr., 7303 CCGC, Ann Arbor, MI 48109-0946, USA
E-mail: cacooper@umicn.edu

men (1). Despite its common occurrence, the biology of prostate cancer and metastasis remains poorly characterized. As a consequence, prostate tumors, after a relatively short period of regression induced by hormone ablation therapy, continue to grow and metastasize to bone and soft tissues. The skeleton is the most common site for prostate cancer metastasis, occurring in more than 80% of advanced prostate cancer patients (2). The proclivity for prostate cancer to metastasize to bone has been explained by a number of theories, including hemodynamic mechanisms, as well as the 'seed and soil' theory (3-5).

It is established that growth factors (GFs) and cytokines involved in cell proliferation and apoptosis can affect the growth of human PCa cell lines (6). In the bone marrow, several GFs and cytokines are produced by osteoblasts and are incorporated into the bone matrix (7). These bone-associated GFs may support and regulate the growth of PCa cells, even in the absence of androgens. The preferential metastasis to bone by PCa cells suggests that factors in the bone may preferentially stimulate PCa cell growth. The current study determines the role of bone-associated GFs and cytokines by comparing their effects on the growth responses of several soft tissue-derived prostate cancer cell lines to the growth responses of several bone-derived prostate cancer cell lines. In total, seven PCa cell lines were studied with eight different GFs and cytokines. We determined that PCa cell lines derived from bone metastases do not respond preferentially to bone-associated GFs and cytokines as compared to PCa cell lines derived from soft tissue metastases. This study suggests that the sensitivity of prostate cancer cells to various GFs and cytokines is heterogenous at various metastatic sites.

Materials and methods

Cell lines and reagents. LNCaP, DU145, and PC-3 human PCa cell lines were purchased from American Type Culture Collection (Rockville, MD). MDA PCa 2a and 2b human PCa cell lines were developed, characterized and kindly provided by Dr Nora Navone (M.D. Anderson Cancer Center, Houston, TX) (8). DuCaP and VCaP were developed in our laboratory and reported (9,10). LNCaP, DU145, and DuCaP were derived from soft tissue metastases, and PC-3, VCaP, MDA PCa 2a and 2b were derived from bone metastases. LNCaP and PC-3 cells were maintained in RPMI-1640 supplemented with

10% fetal bovine serum (FBS) and 1% (vol/vol) penicillin-streptomycin (pen-strep). DU145, DuCaP, and VCaP cells were maintained in DMEM with 10% FBS and 1% pen-strep. MDA PCa 2a and 2b cells were maintained in BRFF-HPC1 media (Biological Research Faculty and Facility, Inc., Jamsville, MD) supplemented with 20% FBS and 1% pen-strep. The culture medium was changed every 3-4 days.

The GFs and cytokines used in this investigation were obtained from two commercially available sources. Recombinant human epidermal growth factor (EGF), recombinant human basic fibroblast growth factor (bFGF), recombinant human tumor necrosis factor-α (TNF-α), recombinant human insulin growth factor-1 (IGF-1), recombinant human platelet-derived growth factor (PDGF), and recombinant human transforming growth factor-ß1 (TGF-ß) were purchased from Gibco (Grand Island, NY). Recombinant human interleukin-6 (IL-6) and recombinant human interleukin-1ß (IL-1ß) were purchased from R&D systems (Minneapolis, MN).

Proliferation assay. All cells were dispersed by trypsin treatment, resuspended in appropriate media (as detailed above) and seeded into 96-well culture plates at various densities (from 5×10^3 cells per well to 1.5×10^4 cells per well) depending on cell type. Twenty-four hours after seeding the cells, attached cells were rinsed with Hank's balanced salt solution, and the media were changed to both normal media (control) and media containing different concentrations of each exogenous GF and cytokine. Forty-eight hours after the addition of each GF and cytokine, 10 μl of WST-1 reagent (Roche, Mannheim, Germany) were added to each well and incubated for 3 h at 37°C. The relative growth rate of each cell line was determined with a microtiter plate reader set at wavelengths of 450 nm and 650 nm. The sample size was 10 for each treatment concentration, and all values were compared to their respective control values. Relative scores were calculated and each experiment was repeated twice.

Statistical analysis. A one-way ANOVA with post hoc test (Scheffe adjustment) was used to determine the significance of various treatments versus the control values. Statistically significant values were indicated by $p < 0.05$.

Results

Human prostate cancer cell lines derived from soft tissue metastases: LNCaP, DU145, and DuCaP. The growth responses of LNCaP, DU145, and DuCaP cells were determined. IGF-1 stimulated LNCaP cell proliferation in a dose-independent manner (Fig. 1A and B). The proliferation of LNCaP cells was significantly decreased with TNF-α treatment (Fig. 1A and C). The TNF-α effect was dose-dependent beyond a concentration of 10 U/ml. No significant growth responses were observed when LNCaP cells were treated with PDGF, bFGF, EGF, IL-6, TGF-ß, and IL-1.

DU145 and DuCaP cells, both derived from dural metastases, demonstrated variable responses to the cytokines. The growth of DU145 cells was significantly increased with treatments using EGF and two lower concentrations of IGF (Fig. 2A and B). No significant growth responses were noted with bFGF, PDGF, TGF-ß, TNF-α, IL-6, and IL-1 treatments
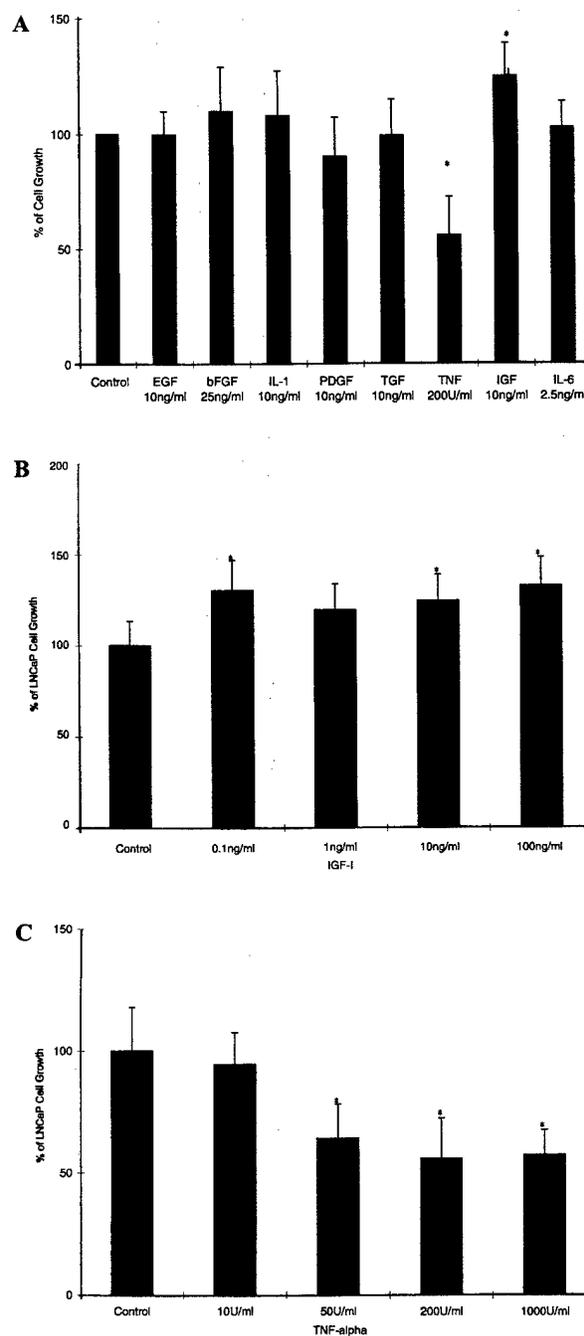
Figure 1. A, The relative growth rate of LNCaP cells incubated for 48 h with each GF/cytokine. B, The growth response of LNCaP cells incubated for 48 h in the presence of 0, 0.1, 1, 10, 100 ng/ml of IGF-1. C, The growth response of LNCaP cells incubated for 48 h in the presence of 0, 10, 50, 200, 1000 U/ml of TNF-α. Results (mean ± SDM) expressed as the percent of the control, with an asterisk indicating significant values (p<0.05) as compared to the control.

(data not shown). The growth of androgen-sensitive DuCaP cells was only significantly affected by IGF treatment at the highest dose (Fig. 2C).

Human prostate cancer cell lines derived from bone metastases: PC-3, MDA-2a, MDA-2b, and VCaP. The effects
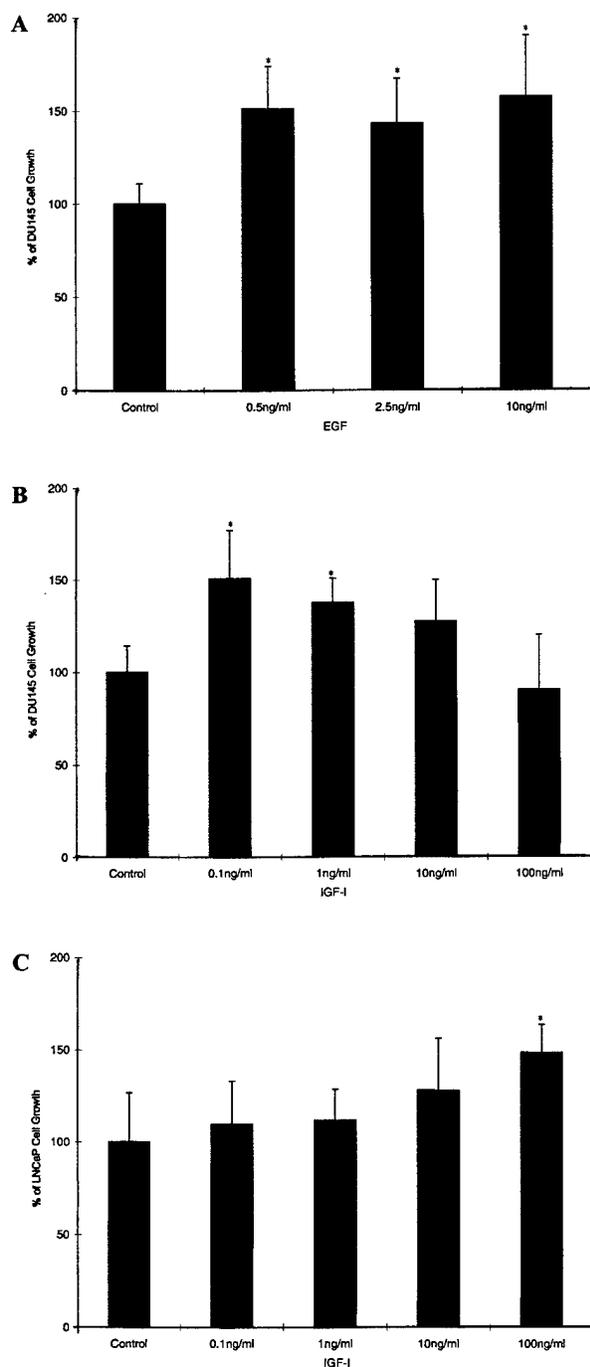
Figure 2. A, The growth response of DU145 cells incubated for 48 h in the presence of 0, 0.5, 2.5, 10 ng/ml of EGF. B, The growth response of DU145 cells incubated for 48 h in the presence of 0, 0.1, 1, 10, 100 ng/ml of IGF-1. C, The growth response of DuCaP cells incubated for 48 h in the presence of 0, 0.1, 1, 10, 100 ng/ml of IGF-1. Results (mean ± SDM) expressed as the percent of the control, with an asterisk indicating significant values (p<0.05) as compared to the control.
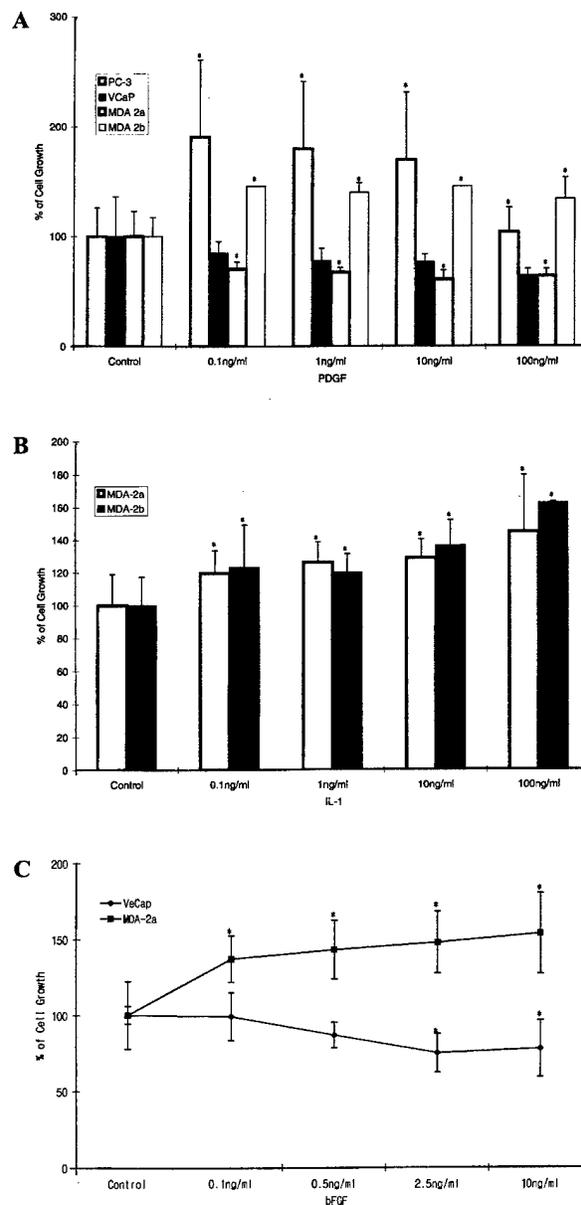

Figure 3. A, The effects of PDGF on the growth of prostate cancer cell lines derived from bone metastases. PC-3 (n=10), VCaP (n=10), MDA-2a (n=10), and 2b (n=10) cells were incubated for 48 h in the presence of 0, 0.1, 1, 10, 100 ng/ml of PDGF. B, The growth responses of MDA-2a and 2b cells incubated for 48 h in the presence of 0, 0.1, 1, 10, 100 ng/ml of IL-I. C, The responses of bFGF on the growth of prostate cancer cells derived from bone metastases. VCaP (n=10) and MDA-2a (n=10) cells were incubated for 48 h in the presence of 0, 0.1, 0.5, 2.5, 10 ng/ml of bFGF. Results (mean ± SDM) expressed as the percent of the control, with an asterisk indicating significant values (p<0.05) as compared to the control.

of bone-associated cytokines on bone-derived prostate cancer cell lines, PC-3, VCaP, MDA-2a and MDA-2b, were evaluated. Among the eight cytokines tested, only PDGF had a significant,

but variable, effect on the growth of all cell lines derived from bone metastases (data not shown). Although it was not statistically significant, the growth of VCaP cells was inhibited by PDGF treatment (Fig. 3A). MDA-2a and MDA-2b cells are newly established cell lines and were derived from the same patient (8). Interestingly, PDGF stimulated the
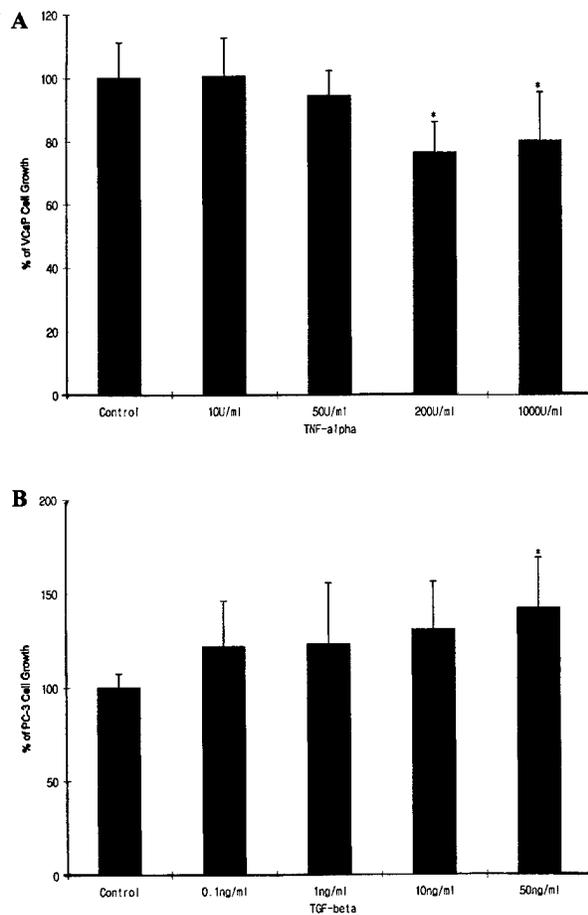
Figure 4. A, The growth response of VCaP cells incubated for 48 h in the presence of 0, 10, 50, 200, 1000 U/ml of TNF-α. B, The growth response of PC-3 cells incubated for 48 h in the presence of 0, 0.1, 1, 10, 50 ng/ml of TGF-ß. Results (mean ± SDM) expressed as the percent of the control, with an asterisk indicating significant values (p<0.05) as compared to the control.

proliferation of MDA-2b cells, but it inhibited the proliferation of MDA-2a cells. PC-3 cell growth was also stimulated significantly (p<0.05) by PDGF (Fig. 3A).

Although PDGF demonstrated a global, yet variable, effect on all cell lines derived from bone metastases, other GFs and cytokines also demonstrated an effect. IL-1 significantly stimulated the growth of MDA-2a and MDA-2b cells (Fig. 3B). VCaP and MDA-2a cells responded to bFGF, but the effects were variable (Fig. 3C). The growth of VCaP cells was significantly inhibited by bFGF at 2.5 ng/ml and 10 ng/ml, while all doses of bFGF stimulated the growth of MDA-2a cells (p<0.05). VCaP cell growth was also reduced by approximately 20% when treated with more than 200 U/ml of TNF-α (p<0.05) (Fig. 4A). Only the higher dose of TGF-ß, 50 ng/ml, significantly stimulated the growth rate of PC-3 cells (p<0.05) (Fig. 4B). The treatments of the four prostate cancer cell lines derived from bone metastases with IGF-1, EGF, and IL-6 did not demonstrate a significant effect (data not shown).

Discussion

IGF-1 is an important growth factor for mesenchymal tissues, including bone and cartilage, and plays an important role in the proliferation of human PCa cell lines (11-13). PC-3, LNCaP, and DU145 cells secrete IGF-1 and have IGF-1 receptors. These cell lines grow by an autocrine loop in which the overproduced IGF-1 activates its receptor (13). Ritchie and colleagues (14), suggested that GFs, such as the IGFs, can increase prostate cell metastasis by stimulating cell division at metastatic sites. The data regarding the role of exogenous IGFs on human PCa cell growth are conflicting. Exogenous IGFs have been shown to stimulate and suppress the proliferation of some PCa cell lines (14-18). The growth rate of LNCaP cells was reportedly decreased by exogenous IGF-1 (13). In this study, exogenous IGF-1 had a stimulatory effect on LNCaP cell growth.

Exogenous PDGF either inhibits or enhances the proliferation of prostate cancer cell lines *in vitro* (13,16, 19,20). In a previous study, exogenous PDGF stimulated the proliferation of PC-3 cells in a dose-dependent manner and overcame dexamethasone's inhibition of PC-3 cell growth (19). The treatment of LNCaP cells with PDGF did not stimulate their growth (20). In our study, PCa cells derived from soft tissue metastases were insensitive to PDGF, whereas PCa cells derived from bone metastases were sensitive to PDGF; however, the sensitivity of these cells to exogenous PDGF was variable, and the expression of PDGF receptors and the exact role of PDGF in PCa cell lines, were not determined.

It has been reported that the androgen-independent PC-3 and DU145 cells produce and are inhibited by TGF-ß, while androgen-responsive LNCaP cells neither produce nor respond to TGF-ß (22). These observations were confirmed in other investigations (14,19-21,23). In the present study, LNCaP cells did not respond to TGF-ß, and this observation is in agreement with earlier publications. In contrast, the growth of PC-3 and DU145 cells was not affected by TGF-ß. Surprisingly, the highest concentration of TGF-ß, which was not used in earlier studies, stimulated the growth of PC-3 cells. Although a reason for the different outcomes is being determined, we speculate that both PC-3 and DU145 may have acquired an inactivating mutation in the gene encoding TGF-ß type I receptor (24), similar to that detected in LNCaP cells that render them insensitive to the effect of TGF-ß. Recently, it was reported that PC-3 and DU145 cells are genetically more unstable than LNCaP cells; therefore, it is conceivable that the PC-3 and DU145 cell lines in our laboratory may have different TGF-ß type I receptor genotypes than those used for previous investigations (24,25).

EGF has been shown to be important in the development of several neoplasms (26). Several human prostate cancer cell lines, including PC-3, LNCaP, and DU145, express EGF and EGF-receptors. Published investigations suggest that auto-crine activation of an EGF-receptor by EGF, regulates PCa cell growth (27,28). MacDonald and Habib (27) concluded that exogenous EGF only minimally affected the growth and DNA synthesis of DU145 cells, whereas LNCaP cell growth was stimulated. In contrast, this study demonstrated that LNCaP cells were insensitive to exogenous EGF, while

DU145 cell proliferation was significantly increased. Interestingly, all the bone-derived PCa cell lines failed to respond to exogenous EGF treatment. The expression of EGF receptors in our cell lines was not determined.

bFGF has been implicated in the osteoblastic response associated with PCa and other tumor cell lines (29,30). Nakamoto and colleagues (31) reported that DU145 and PC-3 cells produced active bFGF and expressed large amounts of bFGF receptors, though only DU145 responded to exogenous bFGF. Other studies observed that PC-3 and DU145 cells were insensitive to exogenous bFGF (16,21) and our data support these observations (16,21). The response of LNCaPs to bFGF is variable, with some studies reporting that bFGF stimulates LNCaP growth (32,33). The current study demonstrated that soft tissue cell lines did not respond to any dose of exogenous bFGF ranging from 0.1 to 10 ng/ml, but among cells derived from bony metastases, there were variable responses to exogenous bFGF. bFGF stimulated MDA-2a cell growth and inhibited VCaP cell growth. Other cells derived from bone metastases were insensitive to exogenous bFGF.

IL-1 receptors are expressed on PCa cell lines and, once, activated by IL-1, can alter their growth (34). Hsieh and Chiao (34) determined that IL-1-induced a dose-dependent growth reduction in LNCaP and JCA-1 cells. Abdul and Hoosein (35) reported that IL-1α mRNA transcripts were expressed in PC-3 and DU145 cell lines but not in LNCaP, MDA-2a, and MDA-2b cell lines. IL-1ß transcripts were expressed only in the PC-3 cell line (35). They also demonstrated that LNCaP cell growth was significantly reduced by low concentrations of IL-1α and ß, but PC-3 and DU145 cells were not affected. Ritchie and colleagues (14) reported that TNF-α, and IL-1ß significantly inhibited the proliferation of LNCaP, DU145, and PC-3 cells. In the current study, only MDA-2a and 2b cells responded to exogenous IL-1ß by demonstrating an increase in their cell growth.

A variety of malignant tumors have been shown to express IL-6, which may use an autocrine loop as a possible mechanism for stimulating cancer cell growth (36-38). LNCaP, DU145, and PC-3 cells have receptors for IL-6, and this cytokine has been reported to inhibit LNCaP cell growth (39,40). Okamoto and colleagues (41) identified possible paracrine and autocrine pathways mediating the IL-6 effect in the LNCaP cell line. They reported that LNCaP cell growth was stimulated by exogenous IL-6 and also suggested that IL-6 functions as a paracrine growth factor for the LNCaP cell line and as an autocrine growth factor for DU145 and PC-3 cell lines. Chung and colleagues (42) reported that IL-6 inhibited the in vitro growth of LNCaP cells, but demonstrated no effect on the growth of PC-3 and DU145 cells. They also concluded that IL-6 appears to undergo a functional transition from paracrine growth inhibitor to autocrine growth stimulator during progression of PCa to the hormone-refractory phenotype. Other studies reported that exogenous IL-6 inhibited growth of LNCaP, PC-3, and DU145 cells (14,43). In our study, the growth of seven PCa cell lines was not modulated by exogenous IL-6.

TNF is a well-characterized secretory product of macrophages that has shown antitumor activity and is being investigated as an important agent in host-mediated antitumor defense (44,45). Sherwood and colleagues (46) demonstrated

that recombinant TNF-α (range 50-200 ng/ml) was cytotoxic to PC-3, DU145, and LNCaP cell lines but not to benign prostatic, epithelial and stromal cell lines in vitro. Other investigations demonstrated that TNF-α was cytotoxic to LNCaP cells but was not cytotoxic to PC-3 and DU145 cells (47-50). Out of seven tested PCa cell lines, only the growth of androgen-sensitive LNCaP and VCaP cells was inhibited by exogenous TNF-α in our study. Recently, several other researchers reported that nuclear factor-κB (NF-κB) had a protective role on TNF-α-induced apoptosis (51,52). Sumitomo and colleagues (47) demonstrated that only TNF-α-induced a slight inhibition in the growth of advanced PCa cell lines (PC-3 and DU145); however, inhibition of NF-κB activity enhanced the ability of TNF-α to induce growth inhibition and apoptotic cell death. Based on our data, we speculate that PCa cell lines, taken from various metastatic sites, are relatively resistant to TNF-α treatment (50).

These results demonstrate that the responses of these cell lines to bone-associated GF and cytokines are variable and depend on the unique phenotype of each cell line and not their metastatic origin nor their expression of the androgen receptor. Prostate cancer metastasis to bone may not be mediated by preferential proliferation in the bone marrow in response to bone-associated GFs and cytokines.

Acknowledgements

References

1. Boring CC, Squires TS, Tong T and Montgomery S: Cancer statistics. CA Cancer J Clin 44: 7-26, 1994.
2. Rubin MA, Putzi M, Mucci N, Smith DC, Wojno K, Korenchuk S and Pienta KJ: Rapid ('Warm') autopsy study for procurement of metastatic prostate cancer. Clin Cancer Res 6: 1038-1045, 2000.
3. Batson OV: The function of the vertebral veins in the metastatic processes. Ann Intern Med 16: 38-45, 1942.
4. Nishijima Y, Uchida K, Koiso K and Nemoto R: Clinical significance of the vertebral vein in prostate cancer metastasis. Adv Exp Med Biol 324: 93-100, 1992.
5. Paget S: The distribution of secondary growths in cancer of the breast. Lancet i: 571-573, 1889.
6. Carruba G, Leake RE, Rinaldi F, Chalmers D, Comito L, Sorci C, Pavone-Macaluso M and Castahneta LA: Steroid-growth factor interaction in human prostate cancer. 1. Short-term effects of transforming growth factors on growth of human prostate cancer cells. Steroids 59: 412-420, 1994.
7. Baylink DJ, Finkelman RD and Moban S: Growth factors to stimulate bone formation. J Bone Miner Res 2 (Suppl 8): S565-S572, 1993.
8. Navone NM, Olive M, Ozen M, Davis R, Troncoso P, Tu SM, Johnston D, Plooack A, Pathak S, von Eschenbach AC and Logothetis CJ: Establishment of two human prostate cancer cell lines derived from a single bone metastasis. Clin Cancer Res 3: 2493-2500, 1997.
9. Lee YG, Korenchuk S, Lehr J, Whitney S, Vessela R and Pienta KJ: Establishment and characterization of a new human prostate cancer cell line: DuCaP. In Vivo 15: 157-162, 2001.
10. Korenchuk S, Lehr J, McLaen L, Lee YG, Whitney S, Vessela R, Lin D and Pienta KJ: VCaP, a cell-based model system of human prostate cancer. In Vivo 15: 163-168, 2001.
11. Schoenle E, Zapf J and Froesch ER: Insulin-like growth factor I and II stimulate growth of hypophysectomozed rats. Diabetologia 23: 199, 1982.
12. Mathews LS, Hammer RE, Behringer RR, D'Ercole AJ, Bell GI, Brinster RL and Palmiter RD: Growth enhancement of transgenic mice expressing human insulin-like growth factor I. Endocrinology 123: 2827-2833, 1988.

13. Pietrzkowski Z, Mulholland G, Gomella L, Jameson BA, Wernicke D and Baserga R: Inhibition of growth of prostatic cancer cell lines by peptide analogues of insulin-like growth factor 1. Cancer Res 53: 1102-1106, 1993.

14. Ritchie CK, Andrews LR, Thomas KG, Tindall DJ and Fitzpatrick LA: The effects of growth factors associated with osteoblasts on prostate carcinoma proliferation and chemotaxis: implications for the development of metastatic disease. Endocrinology 138: 1145-1150, 1997.

15. Kue PF and Daaka Y: Essential role for G protein in prostate cancer cell growth and signaling. J Urol 164: 2162-2167, 2000.

16. Jones HE, Dutkowsk CM, Barrow D, Harper ME, Wakeling AE and Nicholson RI: New EGF-R selective tyrosine kinase inhibitor reveals variable growth responses in prostate carcinoma cell lines PC-3. Int J Cancer 71: 1010-1018, 1997.

17. Cohen P, Peehl DM, Lamson G and Rosenfeld RG: Insulin-like growth factors (IGFs), IGF receptors, and IGF binding proteins in primary cultures of prostate epithelial cells. J Clin Endocrinol Metab 73: 401-407, 1991.

18. Joly-Pharaboz M, Soave M, Nicolas B, Mebarki F, Renaud M, Foury O, Morel Y and Andre JG: Androgens inhibit the proliferation of a variant of the human prostate cancer cell line LNCaP. J Steroid Biochem Mol Biol 55: 67-76, 1995.

19. Reyes-Moreno C, Frenette G, Boulanger J, Lavergne E, Govindan MV and Koutsilieris M: Mediation of glucocorticoid receptor function by transforming growth factor beta I expression in human PC-3 prostate cancer cells. Prostate 26: 260-269, 1995.

20. Chung LW, Li W, Gleave ME, Hseih JT, Wu HC, Sikes RA, Zhau HE, Bandyk MG, Lothesis CJ, Rubin JS and von Eschenbach A: Human prostate cancer model: roles of growth factors and extracellular matrices. J Cell Biochem 16H (Suppl): 99-105, 1992.

21. Okutani T, Nishi N, Kagawa Y, Takasuga H, Takenaka I, Usui T and Wada F: Role of cyclic AMP and polypeptide growth regulators in growth inhibition by interferon in PC-3 cells. Prostate 18: 73-80, 1991.

22. Wilding G, Zugmeier G, Knabbe C, Flanders K and Gelmann E: Differential effects of transforming growth factor ß on human prostate cancer cells *in vitro*. Mol Cell Endocrinol 62: 79-87, 1989.

23. Desruisseau S, Ghazarossian-Ragni E, Chinot O and Martin PM: Divergent effect of TGFbeta1 on growth and proteolytic modulation of human prostatic-cancer cell lines. Int J Cancer 66: 796-801, 1996.

24. Kim IY, Ahn HJ, Zelner DJ, *et al*: Genetic change in transforming growth factor ß receptor type I gene correlates with insensitivity to TGF-ß1 in human prostate cancer cells. Cancer Res 56: 44-48, 1996.

25. Takaha N, Hawkins AL, Griffin CA, Isaacs WB and Coffey DS: High mobility group protein I(Y): a candidate architectural protein for chromosomal rearrangements in prostate cancer cells. Cancer Res 62: 647-651, 2002.

26. Khazaie K, Schirrmacher V and Lichtner RB: EGF receptor in neoplasia and metastasis. Cancer Metastasis Rev 12: 255-274, 1993.

27. MacDonald A and Habib K: Divergent response to epidermal growth factor in hormone sensitive and insensitive human prostate cancer cell lines. Br J Cancer 65: 177-182, 1992.

28. Connolly JM and Rose D: Secretion of epidermal growth factor and related polypeptides by the DU145 human prostate cancer cell line. Prostate 15: 177-186, 1989.

29. Izbicka E, Dunstan CR, Hom D, Harris M, Harris S, Akans R and Mundy GR: Effects of human tumor cell lines on local new bone formation *in vivo*. Calcif Tissue Int 60: 210-215, 1997.

30. Izbicka E, Dunstan C, Esparza J, Jacobs C, Sabatini M and Mundy GR: Human amniotic tumor which induces new bone formation *in vivo* produces a growth regulatory activity *in vitro* for osteoblasts identified as an extended form of basic fibroblast growth factor (bFGF). Cancer Res 56: 633-636, 1996.

31. Nakamoto T, Chang C, Li A and Chodak GW: Basic fibroblast growth factor in human prostate cancer cells. Cancer Res 52: 571-577, 1992.

32. Lecrone V, Li W, Devoll RE, Logothetis C and Farach-Carson MC: Calcirum signals in prostate cancer cells: specific activation by bone matrix proteins. Cell Calcium 27: 35-42, 2000.

33. Hierowski MT, McDonald MW, Dunn L and Sulivan JW: The partial dependency of human prostatic growth factor on steroid hormones in stimulating thymidine incorporation into DNA. J Urol 138: 909-912, 1987.

34. Hsieh TC and Chiao JW: Growth modulation of human prostatic cancer cells by interleukin-1 and interleukin-1 receptor antagonist. Cancer Lett 95: 119-123, 1995.

35. Abdul M and Hoosein N: Differences in the expression and effects of interleukin-1 and -2 on androgen-sensitive and -insensitive human prostate cancer cell lines. Cancer Lett 149: 37-42, 2000.

36. Eustace D, Han X, Gooding R, Rowbottom A, Riches P and Heyderman E: Interleukin-6 (IL-6) functions as an autocrine growth factor in cervical carcinoma *in vitro*. Gynecol Oncol 50: 15-19, 1993.

37. Miki S, Iwano M, Miki Y, Yamamoto M, Tang B, Yokokawa K, Sonoda T, Hirano T and Kishimoto T: Interleukin (IL-6) functions as an *in vitro* autocrine growth factor in renal cell carcinomas. FEBS Lett 250: 607-610, 1989.

38. Tabibzadeh S, Poubouridis D, May LT and Sehgal PB: Interleukin-6 immunoreactivity in human tumors. Am J Pathol 135: 427-433, 1989.

39. Schuurmans ALG, Bolt J, Veldscholte J and Mulder E: Regulation of growth of LNCaP human prostate tumor cells by growth factors and steroid hormones. J Steroid Biochem Mol Biol 40: 193-197, 1991.

40. Siegall CB, Schwab G, Nordan RP, Fitzgerald DJ and Pastan I: Expression of the interleukin 6 receptor and interleukin 6 in prostate carcinoma cells. Cancer Res 50: 7786-7788, 1990.

41. Okamoto M, Lee C and Oyasu R: Interleukin-6 as a paracrine and autocrine growth factor in human prostatic carcinoma cells *in vitro*. Cancer Res 57: 141-146, 1997.

42. Chung TDK, Yu JJ, Spiotto MT, Bartkowski M and Simons JW: Characterization of the role of IL-6 in the progression of prostate cancer. Prostate 38: 199-207, 1999.

43. Mori S, Murakami-Mori K and Bonavida B: Interleukin-6 induces G1 arrest through induction of P27, a cyclin-dependent kinase inhibitor, and neuron-like morphology in LNCaP prostate tumor cells. Biochem Biophys Res Commun 257: 609-614, 1999.

44. Sherwood ER, Williams DL and Diluzio NR: Glucan stimulates production of antitumor cytolytic/cytostatic factors by macrophages. J Biol Response Mod 6: 504-626, 1986.

45. Zeigler-Heibrock HWL, Moller A, Linke RP, Haas JG, Rieber EP and Riethmuller G: Tumor necrosis factor as effector molecule in monocyte-mediated cytotoxicity. Cancer Res 46: 5947-5952, 1986.

46. Sherwood ER, Pitt Ford TR, Lee C and Kozlowski JM: Therapeutic efficacy of recombinant tumor necrosis factor alpha in an experimental model of human prostatic carcinoma. J Biol Response Mod 9: 44-52, 1990.

47. Sumitomo M, Tachibani M, Nakashima J, Murai M, Miyajima A, Kimura F, Hayakawa M and Nakamura H: An essential role for nuclear factor kappa B in preventing TNF-alpha-induced cell death in prostate cancer cells. J Urol 161: 674-679, 1999.

48. Nakajima Y, Dellipizzi AM, Mallouh C and Ferreri NR: TNF-mediated cytotoxicity and resistance in human prostate cancer cell lines. Prostate 29: 296-302, 1996.

49. Nakajima Y, Dellipizzi AM, Mallouh C and Ferreri NR: Effect of tumor necrosis factor-alpha and interferon-gamma on the growth of human prostate cancer cell lines. Urol Res 23: 205-210, 1995.

50. Muenchen HJ, Lin DL, Walsh MA, Keller ET and Pienta KJ: Tumor necrosis factor-α-induced apoptosis in prostate cancer cells through inhibition of nuclear factor-κB by an IkBα super-repressor. Clin Cancer Res 6: 1969-1977, 2000.

51. Beg AA and Baltimore D: An essential role for NF-κB in preventing TNF-α-induced cell death. Science 274: 782-784, 1996.

52. Wang C, Mayo MW and Baldwin AS Jr: TNF- and cancer therapy-induced apoptosis: potentiation by inhibition of NF-κB. Science 274: 784-787, 1996.

Research Paper

In Vivo Visualization of Metastatic Prostate Cancer and Quantitation of Disease Progression in Immunocompromised Mice

Linda M. Kalikin[1]

Abraham Schneider[2]

Melissa A. Thakur[3]

Yaron Fridman[1]

Laura B. Griffin[4]

Rodney L. Dunn[1]

Thomas J. Rosol[5]

Rajal B. Shah[6]

Alnawaz Rehemtulla[4]

Laurie K. McCauley[2,6]

Kenneth J. Pienta[1,3] *

[1]Department of Urology; [3]Department of Internal Medicine, Division of Hematology and Oncology; The University of Michigan Comprehensive Cancer Center; Ann Arbor, Michigan USA

[2]Department of Periodontics, Prevention and Geriatrics; The University of Michigan School of Dentistry; Ann Arbor, Michigan USA

[4]Department of Radiation Oncology; [6]Department of Pathology; The University of Michigan Health System; Ann Arbor, Michigan USA

[5]Department of Veterinary Biosciences; The Ohio State University; Columbus, Ohio USA

*Correspondence to: Kenneth J. Pienta; Department of Internal Medicine, Division of Hematology and Oncology; The University of Michigan Comprehensive Cancer Center; 7303 CCGC; 1500 East Medical Center Drive; Ann Arbor, MI 48109-0946 USA; Tel.: 734.647.3421; Fax: 734.647.9480; Email: kpienta@umich.edu

ABBREVIATIONS

PSA	prostate specific antigen
TRAMP	transgenic adenocarcinoma of the mouse prostate
CCD	charge-coupled device
ROI	region of interest
IP	intraperitoneally
TRAP	tartrate-resistant acid phosphatase

ABSTRACT

While survival periods for patients with localized prostate cancer have increased, there is still no curative therapy for metastatic disease. Using non-invasive bioluminescent imaging, we designed a comprehensive murine model to monitor tumor location and expansion. We detected micrometastases after one week that correlated by gross necropsy, autoradiography, and histopathology with organ and skeletal lesions seen clinically. We calculated in vivo kinetics for tumor growth based on biophoton emissions and observed significantly faster growth of bone lesions and of overall tumor burden in young mice compared to old mice. This model provides a controllable biological system for further investigation into the pathogenesis of metastatic prostate cancer and evaluation of new therapies.

INTRODUCTION

Prostate cancer is the leading noncutaneous malignancy diagnosed in American men and is the second highest cause of cancer mortality in that group.[1] In 2003 it is projected that over 220,000 new cases of prostate cancer will be identified and that almost 29,000 men will die from the disease. Prostate specific antigen (PSA) testing and aggressive surgical and radiation therapies have increased early detection of locally confined disease which have, in turn, vastly extended disease-free survival.[2] Yet despite this progress, a subset of patients harbors minimal residual disease at the time of local therapy and ultimately relapses.[3] Advanced prostate cancer is characterized by distant organ and skeletal metastases that often cause intense pain and morbidity. Hormone ablation is the standard first line therapy for advanced disease; however resistance develops on average after 18-22 months, and at this stage median survival is 9-12 months with no curative clinical recourse currently available.[4]

The design of effective therapies for metastatic prostate cancer has been hampered by the lack of suitable animal models that recapitulate the clinical pathogenesis of this disease. In models such as the TRAMP mouse, in which cancer spontaneously arises in the prostate,[5] and xenografts, in which tumors are experimentally generated in immuno-compromised mice,[6] metastases are often limited to the lungs and lymph nodes. Skeletal metastases, seen in up to 90% of patients with advanced prostate cancer,[7] are more reliably produced in experimental murine models by direct bone injection, by engraftment of human bone, or by serial passaging to generate bone-homing xenograft sub-lines.[8] Tumor analyses in these systems are based on serial sacrifices and require meticulous exploration to locate metastatic lesions.

More recently, the use of in vivo bioluminescence as an optical reporter for tumor cells has greatly enhanced the value of small animals as clinically-relevant models for neoplasia.[9] One of the most versatile systems produces light through the catalysis of luciferin by the firefly *Photinus pyralis* luciferase protein in the presence of ATP and oxygen.[10] Thus, transfection of a luciferase-expressing construct into cancer cell lines provides a bioluminescent marker for each cell and distinguishes it from host murine cells. Tumor biophoton emissions, detectable in vivo using a highly sensitive, charge-coupled device (CCD) camera,[11] are directly proportional to the number of metabolically active cells[12] and are quantifiable.[13] Under anesthesia, animals are reimaged over the course of an experiment, thereby documenting real-time disease progression and minimizing experimental variability. Utilizing the non-invasive and sensitive aspects of the luciferase/luciferin bioluminescence system, we sought to generate a murine model for metastatic prostate cancer that mimicked clinical manifestations and that generated quantifiable results applicable toward future pharmacological testing.

MATERIALS AND METHODS

Cell Lines. PC-3, a spontaneously immortalized cell line derived from a vertebral prostate cancer metastasis, was purchased from American Type Cell Culture (Rockville, MD). Cells were transfected with a luciferase-expressing pLazarus retroviral construct as previously described[14] except that Fugene 6 (Roche Applied Science, Indianapolis, IN) was used per manufacturer's instructions. Parent and transfected cells were cultured in RPMI-1640 supplemented with 10% FBS in a 5% CO_2 humidified chamber.

Mice. Male SCID mice were purchased from Charles River (Wilmington, MA). Mice were housed in specific pathogen free rooms at The University of Michigan AAALAC, International accredited facilities in microisolator cages and were provided ad libitum with food pellets and water. Mice were anesthetized with 1.75% isofluorane/air anesthesia, and two hundred thousand cells in 100 αL of sterile Dulbecco's PBS lacking Ca^{+2} and Mg^{+2} (DPBS) were administered into the left ventricle. Animals were monitored daily.

Imaging. In vivo bioluminescent analysis was conducted through The University of Michigan Small Animal Imaging Resource facility (MSAIR, http://www.med.umich.edu/msair/). Imaging was performed on a cooled CCD IVIS™ system equipped with a 50 mm lens (Xenogen Corp, Alameda, CA), and results were analyzed using the LivingImage® software (Xenogen Corp.). Mice were injected intraperitoneally (IP) with 100 αL of 40 mg/mL luciferin dissolved in sterile DPBS. Ventral images were acquired 15 minutes post injection with an initial integration time of five minutes, binning 10, and f/1. In later weeks, these parameters were adjusted to capture signals below system saturation levels. A mixture of 1.75% isofluorane/air anesthesia was provided through a nose cone delivery system, and animal body temperature was maintained through a heated platform in the chamber during imaging. Pseudo-color images of photon emissions were overlaid on grayscale images of animals to aid in determining spatial distribution of signals. Photon quantitations were calculated within regions of interests (ROIs) from ventral orientations. To image individual organs and bones, anesthetized animals were sacrificed 15 minutes after luciferin IP injection, and organs and bones were rapidly harvested. Whole animal radiographs were taken subsequent to sacrifice on a model MX20 Faxitron XRay Corporation unit (Wheeling, IL). Voltage was set at 23 kV for 7.5 seconds at 2X cabinet level.

Histopathology. At week 7 (young mice) or week 8 (old mice), animals were sacrificed, organs were harvested, and derivative tissue sections were stained with hematoxylin and eosin following routine protocols. Osteoclasts were identified using tartrate-resistant acid phosphatase (TRAP) staining (Sigma, St. Louis, MO) per manufacturer's instructions. Rabbit anti-luciferase antibody (1:3200, Sigma, St. Louis, MO) with EnVision+ Rabbit Peroxidase Kit (DAKO Corp, Carpinteria, CA) was used for immunohistochemistry.

Statistical Analysis. Fisher's Exact Test was used to determine differences in the percentage of mice with metastases at various time points. Mixed regression models were used to determine differences in growth rate and in initial photon value between young and old mice. Growth rate was explored first as a quadratic (curved) effect, then as a linear effect after the curvature was found to not be statistically significant. Interactions were seen between the growth rate and mouse indicator (young versus old) variables to determine whether the shape and rate differed by group. A backward model building selection was used to arrive at the most parsimonious model. All tests were performed at the 5% significance level using the SAS System (Cary, NC).

RESULTS

Correlation of In Vivo Imaging Signals with Necropsy Examinations. To visualize the proliferation of metastatic prostate cancer by bioluminescent technology, PC-3, an established human prostate cancer cell line derived from a bone metastasis, was engineered to express the firefly luciferase protein. A stable transfectant expressing the highest luciferase by Western analysis (PC-3^{Luc}; data not shown) was used for further studies. Twelve young (average seven weeks old) and fourteen old (average 12 months old) male SCID mice were inoculated with cells into the left ventricle, and tumor growth was monitored by weekly imaging using a CCD camera. At one week post-injection, at least one focal photon emission site detected from the ventral side in all (100%) young mice and in nine of fourteen (64%) old mice (p=0.043) provided evidence for micrometastatic locations of PC-3^{Luc} seeding. Bioluminescent-tagged tumor expansion was recorded weekly for seven weeks in the young group and for eight weeks in the old group. Distress from increasing tumor burden, characterized by hunched posture and rough coat, only developed in later weeks. Additionally, a subset of young mice with strong photon emissions at the mandible developed macroscopically visible masses, and a subset of young mice with strong hind limb signals lost the ability to bear weight on these limbs in later weeks. After seven weeks, 11 of 11 young mice (100%) displayed at least one bioluminescent focus, with the twelfth animal dying at week 6. Nine of these 11 mice at week 7 and the mouse that died the previous week (83%) exhibited multiple sites of bioluminescent metastases. After eight weeks, 10 of 13 old mice (77%) showed at least one site of emission, and eight of the 10 mice (62%) demonstrated multiple sites of tumor signals. The fourteenth mouse died at week 7. Three old mice (23%) never produced signals. To correlate external bioluminescent signals with frank lesions, mice were sacrificed, and predicted metastatic locations based on weekly imaging documentation were visually inspected. (Fig. 1) Evidence for soft tissue tumors included enlarged adrenal glands, (Fig. 1E) enlarged lymph nodes, (Fig. 1G) white foci on liver surfaces, and nodules within the lungs on gross inspection. In mice with high bioluminescent hind limb signals, autoradiographs of the proximal tibia, the distal femur, or both contained radiolucent areas characteristic of decreased bone density and lytic lesions and indicated suspected bone metastases. (Fig. 1F) Radiographs of contralateral limbs without photon emissions lacked these features (data not shown). In addition, autoradiographs showed evidence of pathological fractures in hind limb bones from animals presenting with gait problems. Imaging of these isolated organs and bones confirmed them as the bioluminescent signal source seen in the animals. (Fig. 1E-H)

Histopathological Confirmation of Tumor Phenotype. Microscopic examination of soft tissue samples visually affected on gross examination revealed partial to extensive infiltration of tumor cells among normal cells in some organs and distinct adenocarcinoma foci bordered by normal tissue in other organs. (Fig. 2) As well, organs predicted to be affected based on the locations of external bioluminescence signals but which were not visually obvious at necropsy showed histopathological evidence of metastases. For example, bioluminescence of the eyes (Fig. 1D) observed in almost half of young mice specifically linked histologically to metastatic carcinoma of the Harderian gland located behind the orbit. (Fig. 2E) For bone predicted metastases, histological analyses of tibia and femur samples showed significant trabecular destruction along the tumor/bone interface and the presence of TRAP-positive osteoclastic cells, further verifying tumor cytology. (Fig. 3A-C) While autoradiography of the skull was unremarkable, microscopic examination identified mandible and nasal metastases. (Fig. 3E, G) Immunohistochemistry positive cytoplasmic staining for luciferase established the cell line specific origin of the lesions (Fig. 2-right column; Fig. 3D, F, and H). Thus, a combination of gross morphology, radiography, histopathology and immunohistochemistry techniques verified tumors at all sites initially identified by bioluminescence.

Quantitation of Tumor Expansion and Disease Progression. Weekly imaging not only documented individual tumor locations but also captured bioluminescent emission levels. Therefore, biophotons measured within a defined ROI encompassing a recurring site-specific signal directly correlated with tumor size and established rates of tumor expansions when plotted against week post-intracardiac injection. Quantifiable tumors were limited to those with bioluminescent signals spatially isolated from adjacent lesions, thereby avoiding overlapping ROIs. For skeletal lesions, suitable sites included hind limb signals where histopathology showed only a single lesion at the femur or tibia and mandible signals without nasal or eye signals detected on lateral and dorsal imaging views. These bone tumors grew significantly faster in young animals compared to old animals (p<0.001), despite detection of similar photon levels at week 1. (p=0.50; Fig. 4A) For soft tissue tumors, the delineation of ROIs confidently distinct from adjacent signals was limited to one liver tumor and one adrenal gland tumor from two young mice and one
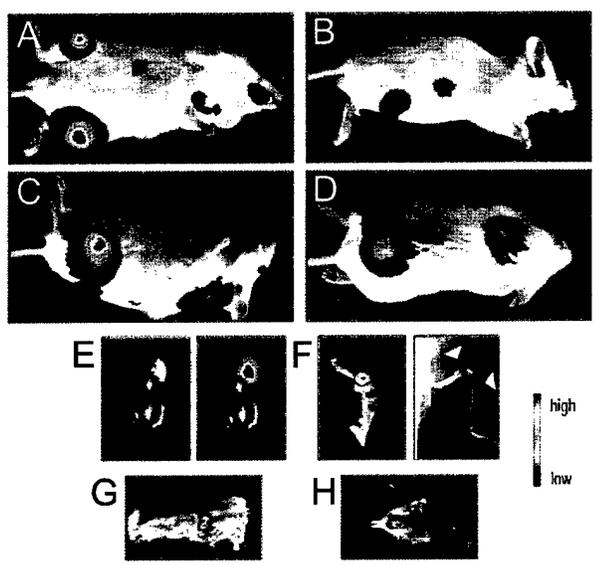
Figure 1. Bioluminescent signals from PC-3[luc] cells are precise indicators for the locations of metastatic lesions. Grey scale images with identically scaled pseudo-color overlays represent rotational views of the same mouse from ventral (A), right lateral (B), dorsal (C), and left lateral orientations at week 7 and aid in identifying tumors at necropsy (E-H). Photon signals at midline in (A, B) coincide with enlarged right adrenal gland (E) shown with attached uninvolved kidney as gray scale (left panel) and pseudo-color overlay (right panel) images. Leg bone emissions (F, left panel) correlate with left hind limb signals in whole animal imaging (A, C, D). White arrowheads in autoradiographic image (F, right panel) indicate osteolytic lesions characteristic of PC-3 cells. Lumbar lymph node (G) and mandible (H) emissions represent lower spine (C) and jaw (A, B) signals respectively. Note that due to poor quality of the isolated mandible for this mouse, (H) is derived from another mouse with similar bioluminescence. Signals from residual cells at the site of intracardiac injection are visible in (A), and emissions at the left scapula (C, D) represent metastatic lymph nodes. A color scale is provided to illustrate relative photon intensities.
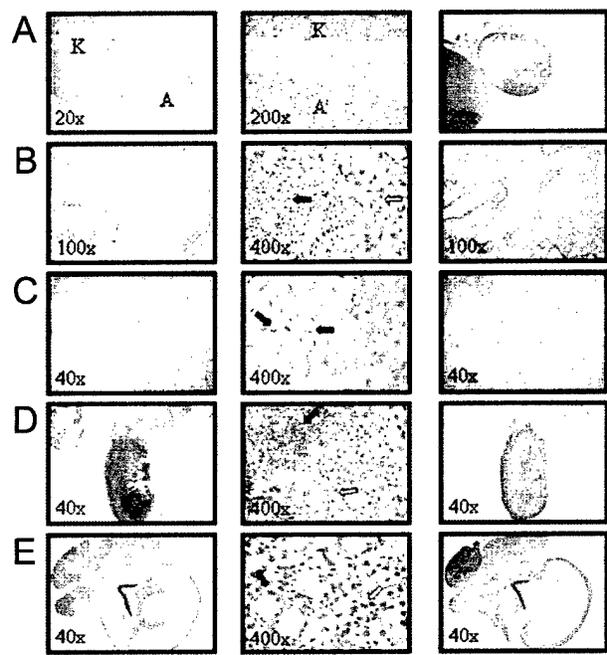

Figure 2. Histology correlates with luciferase immunohistochemical positive staining in soft tissue tumors. Low magnification (left column) of H&E stained sections from representative adrenal gland ((A), adrenal-A with normal kidney-K), lung (B), liver (C), lumbar lymph node (D) and eye (E) shows areas of blue hematoxylin rich tumors. On higher magnification (middle column), characteristic tumor histopathology is evident, including complete replacement of adrenal gland cells by prostate adenocarcinoma cells (A), infiltration of tumor specific cytology among tissue normal cells (B, D; black arrows indicate normal cells, white arrows indicate tumor cells), presence of mitotic figures (C; black arrows), and destruction of normal Harderian gland structure (E; black arrows indicate normal gland, white arrows indicate tumor cells). Expression of luciferase in tumor cells (right column) confirms PC-3 cell line origin.

adrenal gland tumor from an old mouse. While this small sample number precluded the calculation of statistical significance, comparable slopes suggested similar soft tumor growth kinetics within both groups. (Fig. 4B) Total tumor burden, calculated by measuring photon emissions from an ROI encompassing the entire mouse, provided evidence for disease progression. Young mice presented with significantly higher initial tumor burden at week 1 (p=0.01) and exhibited a significantly faster rate (steeper slope) of overall cancer growth compared to old mice. (p<0.001; Fig. 4C)

DISCUSSION

Cancer metastasis is a multiple-step process that requires neovascularization, increased cellular motility, and remodeling of adjacent tissue for primary cancer cells to enter into circulation. Microcolonies establish at distant sites and ultimately develop into macroscopic tumors with additional angiogenesis.[15] Despite significant advances toward early detection of localized prostate cancer, many patients already have occult tumor dissemination to bone marrow and have an increased risk of disease-recurrence at the time of diagnosis.[16] Treatment of metastatic disease with established androgen deprivation therapy successfully leads to stabilization or regression for 80% of patients. However, ultimately all progress to end-stage hormone refractory disease for which only palliative care is available.[4] To address the vital need for improved treatment regimens against metastatic prostate cancer, we developed an in vivo murine model that utilizes bioluminescent tagging of cancer cells and non-invasive imaging technology, thereby permitting sensitive whole body spatiotemporal surveillance and quantitative analyses of tumor growth.

We show that this model rapidly generates micrometastases after one week that can be visualized in vivo with sensitive CCD camera imaging. Moreover, by reimaging the same animals in successive weeks, our model produces real-time in vivo documentation that maps sites of metastases and monitors disease progression. These images are essential for guiding the necropsy examination and for ensuring a more complete analysis of an animal's total tumor burden, whereas in traditional non-tagged xenograft models,[6] small tumors or those at visually inaccessible sites might go undetected. Using intracardiac injection of luciferase-tagged PC-3 cells to mimic systemic circulation of tumor cells after intravasation, we detected metastases at the liver, lungs, lymph nodes, adrenal glands and long bones consistent with metastatic tumors observed from advanced prostate cancer autopsies.[7,17] We also observed mandibular and ocular gland metastases that are highly unusual clinically. We suspect that the high incidence of mandible and nasal bone lesions in this model may be due to the fact that the incisors in mice continuously
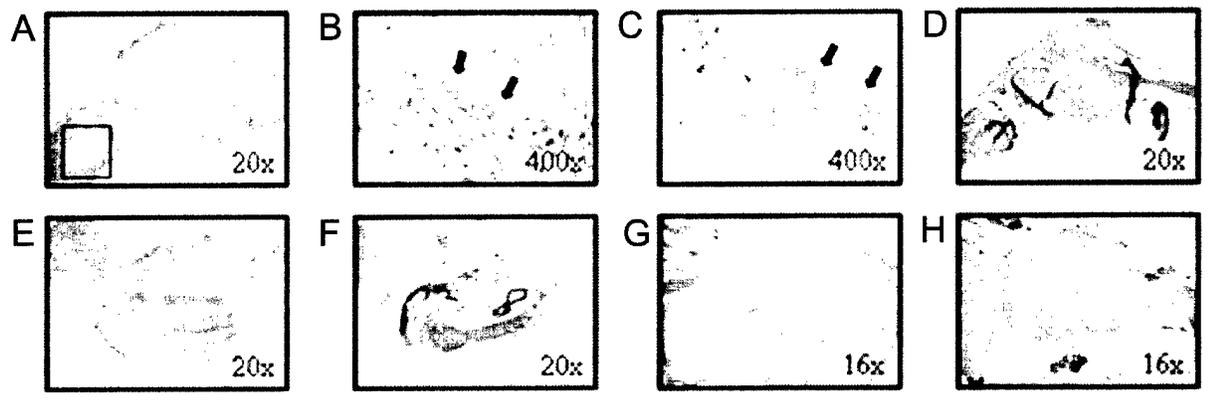
Figure 3. Histological bone lesions contain bone resorbing osteoclasts and express luciferase. Low magnification of H&E stained section from representative femur and tibia (A) shows poorly differentiated carcinoma replacing bone marrow. Evidence of bone destruction at low power is further supported at higher magnification of inset in (A) by the presence of large multi-nucleated osteoclasts (black arrows) at the tumor-bone interface (B) that are positive for TRAP staining (C). Histological staining on representative mandible (E) and nasal (G) bones similarly reveals focally severe carcinoma metastases. Mandible tumor (E) localizes to the labial surface of the incisor. Nasal tumor (G) involves the submucosal compound acinar mucous glands and extends into the skeletal muscle tissue and fascia. On higher magnification, osteoclastic bone resorption is evident in mandible and nasal tumor samples similar to (B) and (C). Tumors stain positive for luciferase expression (D, F, and H), confirming their PC-3 origins.

erupt. Thus, these areas would provide a proliferative microenvironment for tumor cells where bone resorption is a prerequisite.[18] Although we recognize that PC-3 cells are androgen independent, we speculate that the high incidence of metastases to the Harderian gland in this model may be due to the testosterone responsive nature of these glands.[19]

In this model, we also demonstrate the ability to calculate in vivo rates of individual tumor growth and of total tumor burden. These numerical characterizations substantiate our visual observations that bone tumors are more abundant in young mice at earlier weeks but only detected in old mice in the final weeks of imaging. We hypothesize that age related differences in the rate of bone turnover or levels of hormones between these two groups may contribute to this observation.[20] As preliminary evidence also suggests that bone tumor kinetics are comparable to soft tumor growth rates in young mice

but slower in old mice, the significantly faster rate of total tumor burden accumulation in young compared to old mice that we calculated is likely reflective of the differences in bone lesion growth rates between these groups. Biophoton quantification is based on emission spectral qualities which include high transmission and minimal absorbency in living tissue.[11] Used in conjunction with a sensitive, low-noise CCD camera, tumor emitting photon signals detected at the surface of a mouse directly correlate with in vivo tumor volume determined by MRI[12] and can represent as little as several hundred cells.[11] This technology provides a key improvement over other xenograft murine prostate cancer models that monitor fluorescent tagged cells such as with GFP where the required external excitation source contributes to elevated autofluorescent background and to loss of sensitivity.[21] In addition, the ability to reimage animals substantially elevates the inherent experimental reliability for our tumor
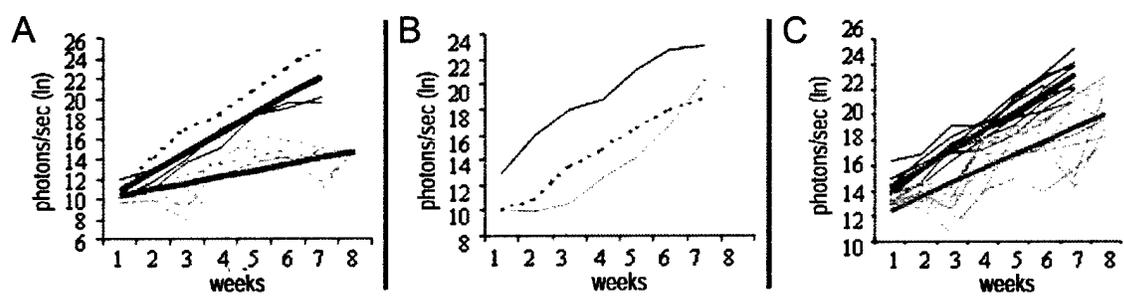

Figure 4. Quantification of tumor growth reveals differences in kinetics between young and old mice. For all graphs (A-C), the natural logs of photon emissions per second from ROIs encompassing bioluminescent signals are represented on the Y axis and are plotted against week post-intracardiac injection on the X axis. Blue lines indicate individual young mice; green lines indicate individual old mice; red lines indicate mean regression calculations. (A) Biophoton emissions from isolated bone tumors increase at a significantly faster rate as illustrated by steeper sloping lines in young animals compared to old animals (p<0.001). Dashed lines represent mandible metastases, and solid lines represent tibia or femur tumors. (B) In contrast, adrenal gland tumor and liver tumor expansions from two young mice and one old mouse appear parallel and therefore suggest similar kinetics between these two groups. Dashed line represents liver tumor, and solid lines represent adrenal gland tumors. (C) The rate of total tumor burden accumulation, calculated as the sum of emission levels from all tumors in an animal at any one time, also occurs significantly faster in young mice compared to old mice (p<0.001).

growth kinetics compared to other calculations derived from serial sacrifice data.[13] Thus, the therapeutic efficacy of novel metastatic prostate cancer treatment strategies can be empirically evaluated, as demonstrated by similar murine bioluminescent models studying treatment strategies in other tumor types.[22]

As spontaneous prostate cancer is an uncommon event in laboratory small animals, spontaneous metastatic prostate cancer in these animals is even more rare. Thus, this model represents a controllable biological system that closely reproduces the clinical progression of metastatic prostate cancer. Notable improvements from previous luciferase-tagged xenograft prostate cancer models include systemic instead of intramuscular or orthotopic inoculation of cancer cells, weekly reimaging of the same animal cohort compared to serial sacrifice, and in vivo emission measurements rather than in vitro luciferase quantitation from tissue homogenates.[13,23] As skeletal metastases are found in almost 90% of patients dying with advanced prostate cancer,[7,17] PC-3 cells were initially optimized in this system due to their high rate of metastases to bone. Their characteristic formation of osteolytic lesions will aid in deciphering the interaction between opposing bone resorption and construction pathways that is thought to contribute to the overall osteoblastic lesions observed in prostate cancer.[24] Simple luciferase retrofitting of additional prostate cancer cell lines for use in this model, such as LNCaP, will allow investigation into other clinical aspects of disease progression including the role of changing PSA production and the formation of osteoblastic bone metastases.

In summary, we describe a murine model that mimics clinically observed bone and soft tissue tumors in minimal to late stage metastatic prostate cancer. Using luciferase-tagged PC-3 cells, sensitive, non-invasive imaging detects early micrometastases later verified by gross examination, histology, autoradiography, and immunohistochemistry and documents real-time disease progression. Calculated growth kinetics illustrate empirically the advantage of using young mice to investigate bone tumorigenesis. This model will be invaluable toward better understanding the systemic pathogenesis of metastatic prostate cancer and toward designing novel therapeutic targets and treatment regiments for future clinical strategies.

References

1. Jemal A, Murray T, Samuels A, Ghafoor A, Ward E, Thun MJ. Cancer statistics, 2003. CA Cancer J Clin 2003; 53:5-26.
2. Hankey BF, Feuer EJ, Clegg LX, Hayes RB, Legler JM, Prorok PC, et al. Cancer surveillance series: Interpreting trends in prostate cancer—part I: Evidence of the effects of screening in recent prostate cancer incidence, mortality, and survival rates. J Natl Cancer Inst 1999; 91:1017-24.
3. Carroll P. Rising PSA after a radical treatment. Eur Urol 2001; 40 Suppl 2:9-16.
4. Pilat MJ, Kamradt JM, Pienta KJ. Hormone resistance in prostate cancer. Cancer Metastasis Rev 1998; 17:373-81.
5. Gingrich JR, Barrios RJ, Morton RA, Boyce BF, DeMayo FJ, Finegold MJ, et al. Metastatic prostate cancer in a transgenic mouse. Cancer Res 1996; 56:4096-102.
6. An Z, Wang X, Geller J, Moossa AR, Hoffman RM. Surgical orthotopic implantation allows high lung and lymph node metastatic expression of human prostate carcinoma cell line PC-3 in nude mice. Prostate 1998; 34:169-74.
7. Rubin MA, Putzi M, Mucci N, Smith DC, Wojno K, Korenchuk S, et al. Rapid ("warm") autopsy study for procurement of metastatic prostate cancer. Clin Cancer Res 2000; 6:1038-45.
8. Rosol TJ, Tannehill-Gregg SH, LeRoy BE, Mandl S, Contag CH. Animal models of bone metastasis. Cancer 2003; 97(3 Suppl):748-57.
9. Edinger M, Cao YA, Hornig YS, Jenkins DE, Verneris MR, Bachmann MH, et al. Advancing animal models of neoplasia through in vivo bioluminescence imaging. Eur J Cancer 2002; 38:2128-36.
10. Timmins GS, Robb FJ, Wilmot CM, Jackson SK, Swartz HM. Firefly flashing is controlled by gating oxygen to light-emitting cells. J Exp Biol 2001; 204:2795-801.
11. Rice BW, Cable MD, Nelson MB. In vivo imaging of light-emitting probes. J Biomed Opt 2001; 6:432-40.
12. Rehemtulla A, Stegman LD, Cardozo SJ, Gupta S, Hall DE, Contag CH, et al. Rapid and quantitative assessment of cancer treatment response using in vivo bioluminescence imaging. Neoplasia 2000; 2:491-5.
13. Rubio N, Villacampa MM, El Hilali N, Blanco J. Metastatic burden in nude mice organs measured using prostate tumor PC-3 cells expressing the luciferase gene as a quantifiable tumor cell marker. Prostate 2000; 44:133-43.
14. Nyati MK, Symon Z, Kievit E, Dornfeld KJ, Rynkiewicz SD, Ross BD, et al. The potential of 5-fluorocytosine/cytosine deaminase enzyme prodrug gene therapy in an intrahepatic colon cancer model. Gene Ther 2002; 9:844-9.
15. Chambers AF, Groom AC, MacDonald IC. Dissemination and growth of cancer cells in metastatic sites. Nat Rev Cancer 2002; 2:563-72.
16. Bianco FJ, Jr., Wood DP, Jr., Gomes de Oliveira J, Nemeth JA, Beaman AA, Cher ML. Proliferation of prostate cancer cells in the bone marrow predicts recurrence in patients with localized prostate cancer. Prostate 2001; 49:235-42.
17. Bubendorf L, Schopfer A, Wagner U, Sauter G, Moch H, Willi N, et al. Metastatic patterns of prostate cancer: an autopsy study of 1,589 patients. Hum Pathol 2000; 31:578-83.
18. Tiffee JC, Xing L, Nilsson S, Boyce BF. Dental abnormalities associated with failure of tooth eruption in src knockout and op/op mice. Calcif Tissue Int 1999; 65:53-8.
19. Ebling FJ, Ebling E, Randall V, Skinner J. The synergistic action of alpha-melanocyte-stimulating hormone and testosterone of the sebaceous, prostate, preputial, Harderian and lachrymal glands, seminal vesicles and brown adipose tissue in the hypophysectomized-castrated rat. J Endocrinol 1975; 66:407-12.
20. Miyaura C, Toda K, Inada M, Ohshiba T, Matsumoto C, Okada T, et al. Sex- and age-related response to aromatase deficiency in bone. Biochem Biophys Res Commun 2001; 280:1062-8.
21. Maeda H, Segawa T, Kamoto T, Yoshida H, Kakizuka A, Ogawa O, et al. Rapid detection of candidate metastatic foci in the orthotopic inoculation model of androgen-sensitive prostate cancer cells introduced with green fluorescent protein. Prostate 2000; 45:335-40.
22. Vooijs M, Jonkers J, Lyons S, Berns A. Noninvasive imaging of spontaneous retinoblastoma pathway-dependent tumors in mice. Cancer Res 2002; 62:1862-7.
23. El Hilali N, Rubio N, Martinez-Villacampa M, Blanco J. Combined noninvasive imaging and luminometric quantification of luciferase-labeled human prostate tumors and metastases. Lab Invest 2002; 82:1563-71.
24. Zhang J, Dai J, Qi Y, Lin DL, Smith P, Strayhorn C, et al. Osteoprotegerin inhibits prostate cancer-induced osteoclastogenesis and prevents prostate tumor growth in the bone. J Clin Invest 2001; 107:1235-44.

3403 Intracardiac injection of luciferase-expressing PC-3 generates a non-invasive *in vivo* model of metastatic prostate cancer progression in immunocompromised mice. Linda M. Kalikin, Abraham Schneider, Laura Griffin, Alnawaz Rehemtulla, Laurie K. McCauley, and Kenneth J. Pienta. *The University of Michigan, Ann Arbor, MI.* Metastatic prostate cancer continues to kill approximately 32,000 men per year in the United States, with 90% of patients dying with disseminated bone disease. While advances in hormonal and chemotherapeutic regimens have extended remission periods, there is still no curative therapy for advanced prostate cancer. We have developed a murine metastatic prostate cancer model utilizing the bioluminescence chemistry of the firefly (*Photuris pyralis*) luciferase enzyme. PC-3, a human osteolytic prostate cancer cell line derived from a bone metastasis, was transfected with a luciferase-expressing retroviral construct, and a stable derivative cell line was used for intracardiac injections into male SCID mice. Following intraperitoneal injections of luciferin, whole body imaging of anesthetized mice was performed using a charge-coupled device (CCD) imaging system. Biophotons generated by the luciferin/luciferase reaction allowed for real-time non-invasive visualization of tumor location and quantitation of tumor growth kinetics. We detected localized signals that increased in magnitude with weekly imaging in 80% of mice studied over 8 weeks. These signals correlated at necropsy and confirmed histologically as tumors of the bone as well as liver, adrenal, and lung and corresponded to similar metastatic sites observed in advanced prostate cancer patients from our rapid autopsy

X 3

CELLULAR, MOLECULAR, AND TUMOR BIOLOGY 16

program at The University of Michigan. In addition, we used photon counts collected from weekly imaging to investigate tumor growth rates. Thus, this model permits serial quantitation of cancer progression from bone and soft tissue organs. It also requires fewer animals for experimentation compared to other systems, thereby reducing experimental variability. We are using this model to evaluate potential drug inhibitors of prostate cancer metastasis. In addition, other prostate cancer cell lines are being modified for luciferase expression including VCaP, an osteoblastic bone-derived prostate cancer cell line developed in our lab. This research is supported by National Cancer Institute SPORE grant 1-P50-CA69568.

In vivo Visualization and Quantitation of Metastatic Bone Disease Progression in SCID Mice.

L. M. Kalikin*[1], A. Schneider[2], M. A. Thakur*[3], L. B. Griffin*[1], A. Rehemtulla*[4], L. K. McCauley[2], K. J. Pienta*[1]. [1]Urology, The University of Michigan, Ann Arbor, MI, USA, [2]Periodontics, Prevention and Geriatrics, The University of Michigan, Ann Arbor, MI, USA, [3]Internal Medicine, The University of Michigan, Ann Arbor, MI, USA, [4]Radiation Oncology, The University of Michigan, Ann Arbor, MI, USA.

Metastatic bone disease develops when cells from primary tumors, especially prostate and breast, enter into circulation and colonize within the skeletal system. These bony tumors have a significant impact on patient quality of life as they generally cause significant pain, reduced function, and poor sleep. Some patients may also experience pathological fractures, hypercalcemia, and spinal cord compressions. As well, treatment side effects may include nausea, constipation, confusion, and fatigue. In 2003, 90% of the almost 29,000 men in the U. S. predicted to die from hormone refractory prostate cancer will also have disseminated bone disease. While disease-free survival periods have steadily increased, there is still no curative therapy for advanced prostate cancer and complications related to distant organ metastases. To gain insight into the pathogenesis of this disease, we developed a murine metastatic prostate cancer model utilizing the bioluminescence chemistry of the firefly (*Photuris pyralis*) luciferase enzyme. Luciferase-tagged PC-3, a human prostate cancer cell line derived from a bone metastasis, was inoculated intracardiac into male SCID mice, and anesthetized animals were imaged weekly in conjunction with intraperitoneal luciferin injections using a CCD camera. Animals were sacrificed after 7 weeks, and 80% presented with histologically confirmed tumors of the tibia, femur, and mandible, all of which colocalized with distinct biophoton imaging signals. Similarly, soft tissue tumors of the adrenals, lymph nodes, liver, and lungs were histologically verified at sites predicted by weekly imaging. Using imaging software, tumor growth rates were calculated by quantifying photon emissions within defined regions of interest, and similar kinetics were demonstrated between bone tumors. Thus, we have generated a non-invasive murine model that allows spatial-temporal visualization and quantitative monitoring of metastatic progression. As mice are reimaged weekly, fewer animals are required, and experimental variability is reduced compared to other models. This model is sensitive enough to detect bone micrometastases as early as one week after intracardiac injection and therefore will be a valuable tool to study the mechanisms of skeletal tumorgenesis and the effectiveness of pharmacological regimens against skeletal colonization by circulating prostate cancer cells.

Disclosures: L.M. Kalikin, None.

M073